UNCLASSIFIED

AD 259 445

Reproduced
by the

ARMED SERVICES TECHNICAL INFORMATION AGENCY
ARLINGTON HALL STATION
ARLINGTON 12, VIRGINIA

UNCLASSIFIED

NOTICE: When government or other drawings, specifications or other data are used for any purpose other than in connection with a definitely related government procurement operation, the U. S. Government thereby incurs no responsibility, nor any obligation whatsoever; and the fact that the Government may have formulated, furnished, or in any way supplied the said drawings, specifications, or other data is not to be regarded by implication or otherwise as in any manner licensing the holder or any other person or corporation, or conveying any rights or permission to manufacture, use or sell any patented invention that may in any way be related thereto.

TR-922

SHAPE OF THE CURRENT OUTPUT PULSE FROM A THIN FERROELECTRIC CYLINDER UNDER SHOCK COMPRESSION

R. H. Wittekindt

15 May 1961

DIAMOND ORDNANCE FUZE LABORATORIES
ORDNANCE CORPS ● DEPARTMENT OF THE ARMY
WASHINGTON 25, D. C.

ORDNANCE CORPS

DIAMOND ORDNANCE FUZE LABORATORIES

WASHINGTON 25, D. C.

Robert W. McEvoy, Lt Col
COMMANDING

W. S. Hinman, Jr.
TECHNICAL DIRECTOR

The Diamond Ordnance Fuze Laboratories is a research, development, and engineering installation under the jurisdiction of the Chief of Ordnance.

The Diamond Ordnance Fuze Laboratories was established by the Ordnance Corps, Department of the Army, on 27 September 1953. The nucleus for these Laboratories was the personnel and facilities of the Ordnance Divisions of the National Bureau of Standards.

Typical fields of activity at the Diamond Ordnance Fuze Laboratories include electronics, physics, mechanics, chemistry, and applied mathematics. Examples of topics under these activities are radiation and field studies, circuit devices, chemical problems, and special electron tube design. The programs include all phases from basic research to product design.

The mission of the Laboratories is to:

1. Conduct research and development in the various physical science and engineering fields directed toward meeting the military characteristics for fuzes and related items.

2. Provide consulting and liaison services as required in connection with the development, production, and use of items developed in the laboratories, or of related items.

3 Fabricate models and prototypes of items under development at the laboratories.

4. Perform developmental testing, including destructive testing of prototypes.

5. Serve as principal Nuclear Radiation Effects Research Group to investigate and determine susceptibility of Ordnance electronic materiel to nuclear weapons radiation environment, mechanisms of those effects, and ways and means of developing less susceptible materiel.

6. Maintain and operate for OCO a special library of technical and progress reports, prepared by Army, Navy, Air Force, and their contractors.

7. Perform the Industrial Engineering Support Mission for all proximity fuze items.

8. Administer the Department of the Army Regional Training Center for the District of Columbia, Virginia, and Maryland region.

DIAMOND ORDNANCE FUZE LABORATORIES
ORDNANCE CORPS WASHINGTON 25, D. C.

DA-5B97-01-005
OMS-5010.11.82600
DOFL Proj 30300

TR-922

15 May 1961

SHAPE OF THE CURRENT OUTPUT PULSE FROM A THIN FERROELECTRIC CYLINDER UNDER SHOCK COMPRESSION

R. H. Wittekindt

FOR THE COMMANDER:
Approved by

Israel Rotkin
Israel Rotkin
Chief, Laboratory 300

CONTENTS

LIST OF SYMBOLS IN ORDER OF APPEARANCE IN THE TEXT

A = area of one electrode

ℓ = thickness of the element

P_o = remnant polarization of the element

Q_o = $A\ P_o$ = initial charge on the electrodes

U = voltage

E = electric field strength

i = Index for initial state (before the shock front)

f = index for final state (behind the shock front)

t = time

t_o = ℓ/u_s = normal pulse length

u_s = velocity of the shock front

I = current output

R = resistive load (ohmic resistor)

L = inductive load (inductance of the resistor and the wires)

ξ = $u_s t$ = position of the shock front at the time t

σ = charge density on the electrodes

Q = $\sigma \cdot A$ = total charge on the electrodes (as a function of time)

D = Electric displacement = σ in the practical system

ϵ_o = dielectric constant of free space

ϵ_f = dielectric constant behind the shock front

ϵ_i = dielectric constant before the shock front (mean value)

S = $\epsilon_i/\epsilon_f - 1$ = shape factor

α = dielectric constant before the shock front, for low field E_i

β = coefficient for the quadratic fit to the hysteresis curve

ϵ_m = dielectric constant before the shock front (maximum value for coercive force field, $E = -E_c$)

$-E_c$ = coercive force in the uncompressed material

x = t/t_o = normalized time

y = $I\ t_o/Q_o$ = normalized current

M = $(t_o \ell)/(\epsilon_i\ AR)$

F = $M(x + x^2 S/2)$

ω_o = $\sqrt{M/(2S)}$

ω = $\omega_o(1+Sx)$

$T = (R\, t_o)/(2L)$

$N = (\ell t_o^2)/(\epsilon_i\, LA)$

$\gamma = (1 - x)/x$

$\phi(x)$ = auxiliary function

C = capacitance

W = energy output

r = total resistance of the compressed material

ρ = resistivity of the compressed material

$\bar{\sigma}$ = charge density, diminished by conduction

$\eta = t_o/(\epsilon_f \rho) = t_o(1+S)/(\epsilon_1 \rho)$

$2r$ = diameter of the element

ζ = position along this diameter

φ = angle of impact

t_a = time delay due to the angle of impact

$z = t_a/t_o$ = normalized time delay

B = abbreviation for equation (72)

T = abbreviation for equation (74)

x_p = position of the peak of the output curve $y(x)$

ABSTRACT

When a polarized ferroelectric element is traversed by a shock front that destroys the polarization, a current output appears. The shape of the curve of this current output versus time is computed in a normalized and general form for the case where the shock front moves in a direction normal (or approximately normal) to the electrodes and parallel to the polarization. The influence of the external electric load, of the dielectric constants and the hysteresis, of a conductivity in the compressed material, and of an oblique impact is discussed. The condition for maximum energy output also is discussed. Mathematical expressions for the current output are given for the various conditions, examples are calculated and shown in graphs. Methods are described for evaluating the dielectric constant in the compressed material from measured output curves.

1. INTRODUCTION

The calculations reported evolved from the need to evaluate certain experimental results. The topic, experimental setup, and first results are described by P.S. Brody in reference 1, in which he states the basic theoretical expression for the current output under shock compression, when a shock front travels through an axially polarized ferroelectric disc in the direction of its polarization. In the present report, the theoretical expression (transformed into a more convenient and general "normalized form") is examined in terms of its various parameters. New parameters are added -- the curvature of the hysteresis curve, the inductive load, the conductivity behind the shock front, and the angle of impact. In certain cases the formulas can be solved for ϵ_f, the dielectric constant of the compressed material. The latter, therefore, can be calculated from measured output curves.

The assumptions are:

1) The shock front is very thin, that is: pressure, temperature, particle velocity, and dielectric constant reach their new values within a time short compared with the total pulse length.

2) No relaxation time with respect to the change in polarization appears. The polarization goes to zero immediately after the material is in its high pressure state.

3) The material is isotropic.

4) No reflected rarefaction or compression waves from the edges or from the back surface of the element appear in time to disturb the process.

5. The uncompressed material (before the shock front) follows a hysteresis curve, which can be measured for elements of the same type, and for which therefore a numerical fit can be made for the purpose of evaluating measured output curves.

6) The "dielectric constant" of the compressed material (behind the shock front) is supposed to be a constant, ϵ_f, with respect to the field, E_f. If this assumption is not true for a large field (which we do not know), then the early part of the output pulse will be different from that shown in this report. The tail of the pulse, however, depends on ϵ_f for a small field, when it is more likely to be constant.

2. CURRENT OUTPUT AS A FUNCTION OF TIME

In order to set up an equation for the current output, the following physical process is described: Initially the whole element is polarized, the value of the polarization is P_o. A free charge $\pm Q_o$ ($= A \cdot P_o$) has been allowed to accumulate on the electrodes, kept in place by the polarization and neutralizing its effect. The net field is zero (fig. 1a). After an impact has occurred, a shock front travels through the element, leaving behind a cubic lattice with no spontaneous polarization. During this time the charge from the electrodes flows off. The internal polarization in the undisturbed region is no longer completely neutralized; an increasing field E_i appears here in the negative direction. In the compressed region with no spontaneous polarization, a field E_f in the positive direction appears as a result of the external charge on the electrodes. E_f decreases with time as the charge does (fig. 1b). Finally the shock front has passed the element. There remains a decreasing field E_f as long as a charge remains on the electrodes (fig. 1c).

Because the thickness of the element is small compared with its diameter, and because the dielectric constants in the material are much larger than in free space, edge effects can be neglected. The sum of voltages along a closed loop must be zero. So we get (see fig. 1b):

$$E_f \cdot \xi + E_i \cdot (\ell - \xi) - I \cdot R - L \frac{dI}{dt} = 0. \qquad (1)$$

E_i is negative. The current I, in the direction shown, is the negative derivative of the charge Q with respect to time (since the charge decreases with time). In the practical system the charge density σ equals the dielectric displacement, $\sigma = D$. D is connected to E in the following ways: For the compressed material we assume a linear relationship, employing ϵ_f, the dielectric constant behind the shock front,

$$D = \epsilon_f E_f , \qquad (2)$$

from which follows

$$E_f = \frac{D}{\epsilon_f} = \frac{\sigma}{\epsilon_f} .$$

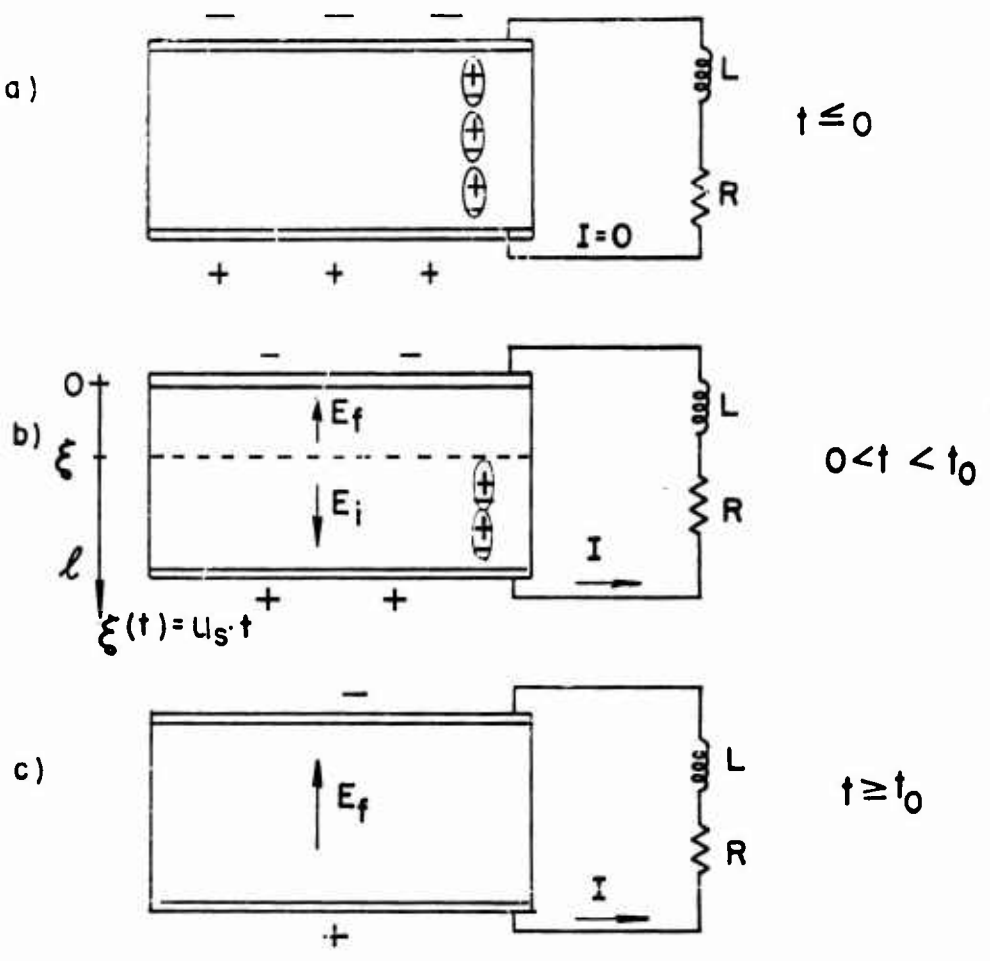

Figure 1. Fields, charge, and current, as the shock front moves through the element.

The uncompressed material before the shock front follows a hysteresis curve. We are interested in its second quadrant only.

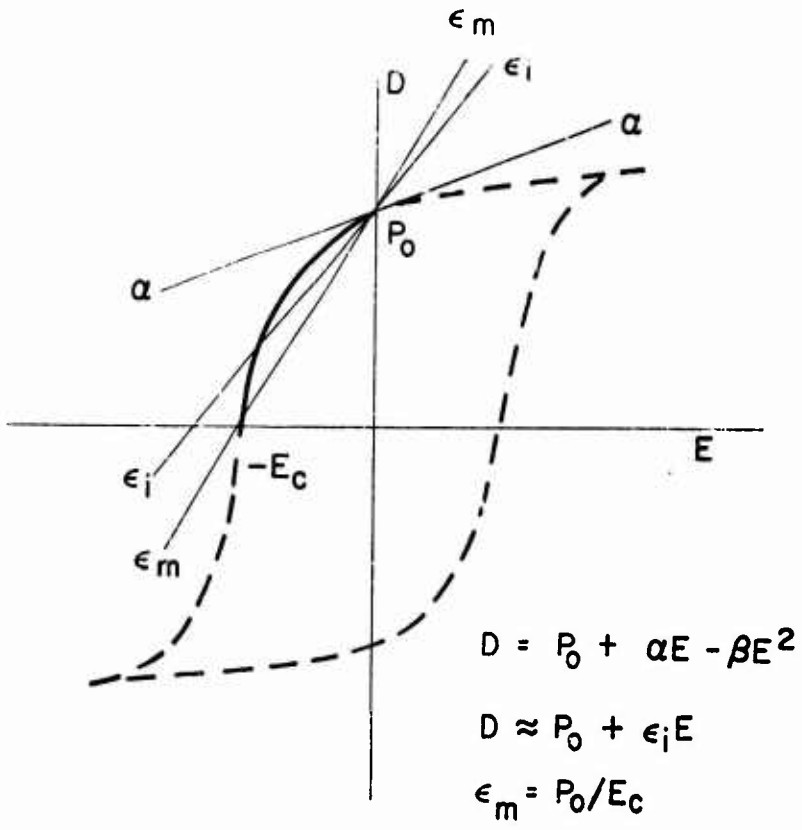

Figure 2. Hysteresis curve in the uncompressed material.

For a very small field E we find the relation*

$$D = P_o + \alpha E,$$

α is the apparent dielectric constant when measured with a low field bridge. With increasing field E in the negative direction, the dielectric constant $\frac{\Delta D}{\Delta E}$ is no longer constant but increases also, and reaches its maximum value ϵ_m for the field $-E_c$ (coercive force). In a simplified manner the hysteresis curve can be approximated by a (somewhat arbitrary) mean value ϵ_i, giving

* The difference between polarization P and dielectric displacements D is neglected since ϵ_i is very large.

$$D = P_o + \epsilon_i E_i \quad , \tag{3}$$

from which follows

$$E_i = - \frac{P_o - D}{\epsilon_i} = - \frac{P_o - \sigma}{\epsilon_i} \quad .$$

A better approach is accomplished with a second order fit,

$$D = P_o + \alpha E_i - \beta E_i^2 \quad , \tag{4}$$

from which follows

$$E_i = - \frac{\alpha}{2\beta} \left(\sqrt{1 + \frac{4\beta}{\alpha^2} (P_o - \sigma)} - 1 \right) \quad .$$

The current is

$$I = - A \frac{d\sigma}{dt} = - A\dot{\sigma} = - \dot{Q} \quad ,$$

and the distance traveled by the shock front is $\xi = u_s t$. Combining (1) with (2) and (3) results in

$$\frac{Q}{\epsilon_f} u_s t - \frac{[Q_o - Q]}{\epsilon_i} (\ell - u_s t) + AR\dot{Q} + AL\ddot{Q} = 0 \tag{5}$$

This is a differential equation of charge Q as a function of time t. From its solution one gets the current $I = - \dot{Q}$ as a function of time. P_o, ϵ_i, ϵ_f, ℓ, u_s, R, A are constant experimental values or parameters. The initial values are $Q = Q_o$ for $t = 0$ and $\dot{Q} = 0$ for $t = 0$.

Since this report deals with the general theory and the influence of certain parameters rather than with specific values from experiments, it is convenient to eliminate some geometrical and experimental parameters by introducing a normalized form. Nothing is lost with it, since any specific values always can be introduced again into the resulting equations. Normalization in this sense is achieved by normalized units of time, charge, and current. The unit of time is

$$t_o \left(= \frac{\ell}{u_s}\right),$$

the time required for a shock to traverse the element. The unit of charge is Q_o, the initial charge bound to the electrodes by the polarization of the element. The unit of current is the quotient $\frac{Q_o}{t_o}$. So we get the normalized time

$$x = \frac{t}{t_o}$$

which goes from zero to one (except under an oblique impact, where $0 < x < 1 + z$), and the normalized current output

$$y = \frac{t_o}{Q_o} I = -\frac{t_o}{Q_o} \frac{dQ}{dt} = -\frac{1}{Q_o} \frac{dQ}{dx} \tag{6}$$

Most graphs in this report show the function y(x).

Equation (5) multiplied by $\frac{\epsilon_i}{\ell}$ gives

$$-Q_o(1-x) + Q\,(1+S\,x) + \dot{Q}\,\frac{\epsilon_i AR}{\ell} + \ddot{Q}\,\frac{\epsilon_i AL}{\ell} = 0 \tag{7}$$

with $S = \frac{\epsilon_i}{\epsilon_f} - 1$ = "shape factor".

In order to use the normalized time x rather than t, we have to transform

$$\dot{Q} = \frac{1}{t_o} \frac{dQ}{dx}\ , \quad \ddot{Q} = \frac{1}{t_o^2} \frac{d^2Q}{dx^2}\ ,$$

giving

$$-Q_o(1-x) + Q\,(1+S\,x) + \frac{dQ}{dx} \frac{\epsilon_i AR}{t_o \ell} + \frac{d^2Q}{dx^2} \frac{\epsilon_i AL}{t_o^2 \ell} = 0\ . \tag{8}$$

This is the general differential equation for Q(x), the initial values are $Q = Q_o$ and $\frac{dQ}{dx} = 0$ for $x = 0$. Once the solution Q(x) has been found, the normalized current output y(x) is computed by

$$y = -\frac{1}{Q_o} \frac{dQ}{dx}\ . \tag{6}$$

For the case $R = 0$, $L = 0$, (short circuit) we get

$$Q = Q_o \frac{1-x}{1+Sx} \tag{9}$$

$$y = \frac{1+S}{(1+Sx)^2}\ . \tag{10}$$

For the case $R \neq 0$, $L = 0$ we get from (8)

$$\frac{dQ}{dx} + Q\,(1 + S\,x)\,M - Q_o(1 - x)\,M = 0$$

with

$$M = \frac{t_o \ell}{\epsilon_i AR} \tag{11}$$

A rather simple solution exists if $S = 0$ (or $\epsilon_i = \epsilon_f$), namely

$$Q = Q_o\left(1 - x + \frac{1}{M} - \frac{e^{-Mx}}{M}\right), \tag{12}$$

from which follows

$$y = 1 - e^{-Mx}, \tag{13}$$

and the initial slope is

$$\left(\frac{dy}{dx}\right)_{x=0} = M = \frac{t_o \ell}{\epsilon_i AR}. \tag{14}$$

If $S \neq 0$, the general solution to (11) follows the scheme:

$$Q' + Q\, f(x) - g(x) = 0$$

$$Q = e^{-F}\left(Q_o + \int_0^x g(x)\, e^{F}\, dx\right)$$

with $$F = \int_0^x f(x)\, dx .$$

Here we have

$$F = M\left(x + \frac{S}{2} x^2\right), \quad \text{and thereby}$$

$$Q = Q_o\, e^{-F}\left[1 + M\int_0^x (1 - x)\, e^{F}\, dx\right], \tag{15}$$

$$y = M\left[(1+S\,x)\, e^{-F} + M(1+Sx)\, e^{-F}\int_0^x (1-x)\, e^{F}\, dx - 1 + x\right]. \tag{16}$$

The integral cannot be solved analytically; however, by partial integration another form can be derived:

$$y = M\,\frac{1+S}{S}\left[(1+Sx)\, e^{-F} + M(1+Sx)\, e^{-F}\int_0^x e^{F}\, dx - 1\right]. \tag{16a}$$

A third form of the solution can be derived from (16) by these definitions:

$$\omega_o = \sqrt{\frac{M}{2S}} \quad \text{and} \quad \omega = \omega_o(1+Sx)$$

from which follow

$$d\omega = S\omega_o \, dx = \sqrt{\frac{MS}{2}} \, dx$$

$$F = M\left(x + \frac{S}{2} x^2\right) = \omega^2 - \omega_o^2$$

$$1 - x = \frac{1+S}{S} - \frac{1}{S} \frac{\omega}{\omega_o}$$

$$1 + Sx = \frac{\omega}{\omega_o}$$

$$y(x) = y\left(\omega(x)\right) = y(\omega)$$

$$y(\omega) = M\left[\frac{\omega}{\omega_o} e^{-(\omega^2-\omega_o^2)} - \frac{1+S}{S} + \frac{1}{S} \frac{\omega}{\omega_o}\right.$$

$$\left. + M \frac{\omega}{\omega_o} e^{-(\omega^2-\omega_o^2)} \int_{\omega_o}^{\omega} \left(\frac{1+S}{S} - \frac{1}{S} \frac{\omega}{\omega_o}\right) e^{\omega^2-\omega_o^2} \frac{1}{S\omega_o} \, d\omega\right]$$

which after some manipulations, leads to

$$y(\omega) = M \frac{1+S}{S}\left[\frac{\omega}{\omega_o} e^{-(\omega^2-\omega_o^2)} + 2\omega e^{-\omega^2} \int_{\omega_o}^{\omega} e^{\omega^2} \, d\omega - 1\right] . \qquad (16b)$$

Solution (16b) is given in reference 1. Its advantage is that the term $e^{-\omega^2} \int_0^{\omega} e^{\omega^2} d\omega$ can be found tabulated, at least in a certain range of ω.

The initial slope can be calculated from any of these forms, giving

$$\left(\frac{dy}{dx}\right)_{x=0} = M(1 + S) = \frac{\ell t_o}{\epsilon_f RA} \qquad (17)$$

Equation (17) includes equation (14) for $S = 0$. Transformed back to the observable output curve $I(t)$, we have as the initial slope for any S:

$$\left(\frac{dI}{dt}\right)_{t=0} = -\frac{Q_o}{t_o} \frac{\ell}{\epsilon_f RA} . \qquad (18)$$

It is interesting to note that the initial rise of the curve voltage (across R) versus time is independent of R,

$$\left(\frac{dU}{dt}\right)_{t=0} = - \frac{Q_o}{t_o} \frac{\ell}{\epsilon_f A} . \tag{19}$$

This is all for the case $R \neq 0$, $L = 0$.

For the case $R = 0$, $L \neq 0$ we get from (8):

$$\frac{d^2Q}{dx^2} + N (1 + Sx) Q - N (1 - x) Q_o = 0 \tag{20}$$

with

$$N = \frac{\ell t_o^2}{\epsilon_i LA} .$$

A solution can be found if $S = 0$, namely

$$Q = Q_o (1 - x + \frac{1}{\sqrt{N}} \sin \sqrt{N} x) \tag{21}$$

$$y = 1 - \cos \sqrt{N} x \tag{22}$$

$$\left(\frac{dy}{dx}\right)_{x=0} = 0. \tag{23}$$

Equation (23) is true for any S, since it is a consequence of (20).

For the general case $R \neq 0$, $L \neq 0$ we get from (8):

$$\frac{d^2Q}{dx^2} + 2T \frac{dQ}{dx} + N (1 + Sx) Q - N (1 - x) Q_o = 0 \tag{24}$$

with

$$T = \frac{Rt_o}{2L}$$

and

$$N = \frac{\ell t_o^2}{\epsilon_i LA}$$

Solutions can be found if $S = 0$, namely

a) for $T^2 < N$, $\frac{R^2}{L} < \frac{4\ell}{\epsilon_i A}$, with $\sqrt{N - T^2} = \phi$

$$Q = Q_o \left[\frac{2T+N}{N} - x - e^{-Tx} \frac{T^2-\phi^2}{N\phi} \sin \phi x - e^{-Tx} \frac{2T}{N} \cos \phi x \right] \quad (25a)$$

$$y = 1 - e^{-Tx} \frac{T}{\phi} \sin \phi x - e^{-Tx} \cos \phi x , \quad (26a)$$

b) for $T^2 = N$, $\frac{R^2}{L} = \frac{4\ell}{\epsilon_i A}$

$$Q = Q_o \left[\frac{2+T}{T} - x - e^{-Tx} \left(x + \frac{2}{T}\right) \right] \quad (25b)$$

$$y = 1 - e^{-Tx} (Tx + 1) \quad (26b)$$

c) for $T^2 > N$, $\frac{R^2}{L} > \frac{4\ell}{\epsilon_i A}$, with $\sqrt{T^2 - N} = \theta$

$$Q = Q_o \left[\frac{2T+N}{N} - x - \frac{T+\theta}{2\theta(T-\theta)} e^{-(T-\theta)x} + \frac{T-\theta}{2\theta(T+\theta)} e^{-(T+\theta)x} \right] \quad (25c)$$

$$y = 1 - e^{-Tx} \left[\frac{T+\theta}{2\theta} e^{\theta x} - \frac{T-\theta}{2\theta} e^{-\theta x} \right]. \quad (26c)$$

The initial slope is, as a consequence of equation (24),

$$\left(\frac{dy}{dx}\right)_{x=0} = 0, \quad (27)$$

and therefore is true for any S.

So far the calculations have involved the simplified formula (3) for the hysteresis in the uncompressed material. There has also been given a better approximation to the curved hysteresis with formula (4). The reasons for using the simplified formula (3) at all, is that with formula (4) the mathematical expressions become very clumsy, the calculations cannot be pushed so far, and, on the other hand, many basic features can be demonstrated adequately by the simpler formulas. However, it is necessary to see how the formulas and the current-output curves actually look when the curvature of the hysteresis is taken into account better. Because of the mathematical difficulties, this will be done for the case R = 0, L = 0 only.

Instead of equation (5) we get by combining (1) with (2) and (4):

$$\frac{\sigma}{\epsilon_f} u_s t - \frac{\alpha}{2\beta}\left[\sqrt{1 + \frac{4\beta}{\alpha^2}(P_o - \sigma)} - 1\right](\ell - u_s t) = 0. \qquad (28)$$

Compared with equation (5), the last two terms involving R and L have been dropped already.

The relation $\ell = u_s t_o$ is used and the time is normalized, $x = t/t_o$, giving

$$\frac{\sigma}{\epsilon_f} x - \frac{\alpha}{2\beta}\left[\sqrt{1 + \frac{4\beta}{\alpha^2}(P_o - \sigma)} - 1\right](1 - x) = 0 . \qquad (29)$$

For $x = 0$, we have $\sigma = P_o$ and therefore from (4): $E_i = 0$, and from (2):

$$E_f = \frac{P_o}{\epsilon_f} .$$

For $x \neq 0$, (29) is rearranged to

$$\sigma^2 + \sigma\frac{\epsilon_f\gamma(\alpha + \epsilon_f\gamma)}{\beta} = P_o\frac{\epsilon_f^2\gamma^2}{\beta}$$

with the solution

$$\sigma = \frac{\epsilon_f\gamma(\alpha+\epsilon_f\gamma)}{2\beta}\left[\sqrt{1 + \frac{4\beta P_o}{(\alpha+\epsilon_f\gamma)^2}} - 1\right] , \qquad (30)$$

including the abbreviation $\gamma = \frac{1-x}{x}$.

Equation (30) gives the charge per unit area remaining on the electrodes as a function of time (t, or $x = t/t_o$, or $\gamma = \frac{1-x}{x}$).

For the very first part of the pulse, that is for x very small and $\gamma \approx \frac{1}{x} \to \infty$, a simplified formula instead of (30) can be deduced. The root is expanded according to the scheme

$$\sqrt{1 + z} = 1 + \frac{z}{2} - \frac{z^2}{8}$$

giving

$$\sigma = P_o\frac{1}{1 + \frac{\alpha}{\epsilon_f\gamma}} - P_o^2\frac{\beta}{\epsilon_f^2\gamma^2\left(1 + \frac{\alpha}{\epsilon_f\gamma}\right)^3} ,$$

which in turn is expanded again. Dropping all terms with factors of order greater than x^2, we obtain

$$\sigma = P_o - P_o \frac{\alpha}{\epsilon_f} x - P_o^2 \frac{\beta}{\epsilon_f^2} x^2 \quad .$$

The complete solution thus is:

$$\begin{cases} \sigma = P_o, & \text{for } x = 0 \\ \sigma = P_o - P_o \dfrac{\alpha}{\epsilon_f} x - P_o^2 \dfrac{\beta}{\epsilon_f^2} x^2, & \text{for } x \text{ very small} \\ \sigma = \dfrac{\epsilon_f \gamma(\alpha+\epsilon_f\gamma)}{2\beta}\left[\sqrt{1+\dfrac{4\beta P_o}{(\alpha+\epsilon_f\gamma)^2}} - 1\right], & \text{for } x < x \leq 1 \\ \sigma = 0, & \text{for } x = 1 \quad . \end{cases} \tag{31}$$

Now the fields can be calculated. Using equation (2) and (31) we get

$$\begin{cases} E_f = \dfrac{P_o}{\epsilon_f}, & \text{for } x = 0 \\ E_f = \dfrac{P_o}{\epsilon_f} - P_o \dfrac{\alpha}{\epsilon_f^2} x, & \text{for } x \text{ very small} \\ E_f = \dfrac{\gamma(\alpha+\epsilon_f\gamma)}{2\beta}\left[\sqrt{1+\dfrac{4\beta P_o}{(\alpha+\epsilon_f\gamma)^2}} - 1\right], & \text{for } 0 < x \leq 1 \\ E_f = 0, & \text{for } x = 1^* \quad . \end{cases} \tag{32}$$

E_i is defined by equation (4). We take advantage of equation (29), which is nothing but $E_f x + E_i (1 - x) = 0$, or $E_i = -1/\gamma\, E_f$.

$$\begin{cases} E_i = 0, & \text{for } x = 0 \\ E_i = -\dfrac{P_o}{\epsilon_f} x, & \text{for } x \text{ very small} \\ E_i = -\dfrac{\alpha+\epsilon_f\gamma}{2\beta}\left[\sqrt{1+\dfrac{4\beta P_o}{(\alpha+\epsilon_f\gamma)^2}} - 1\right], & \text{for } 0 < x \leq 1 \\ E_i = -\dfrac{\alpha}{2\beta}\left[\sqrt{1+\dfrac{4\beta P_o}{\alpha^2}} - 1\right], & \text{for } x = 1, \end{cases} \tag{33}$$

with $\gamma = \dfrac{1-x}{x}$.

*$\sigma = 0$ and $E_f = 0$ for $x = 1$ is typical for the short circuit case ($R = L = 0$).

The charge is $Q = A\sigma$, and therefore is given by (31). The normalized current is

$$y(x) = -\frac{1}{Q_o}\frac{dQ}{dx} = -\frac{1}{P_o}\frac{d\sigma}{dx} = \frac{1}{P_o x^2}\frac{d\sigma}{d\gamma}$$

or from equation (31):

$$\begin{cases} y = \dfrac{\alpha}{\epsilon_f}, & \text{for } x = 0 \\ y = \dfrac{\alpha}{\epsilon_f} + P_o \dfrac{2\beta}{\epsilon_f^2} x, & \text{for } x \text{ very small} \\ y = \dfrac{\epsilon_f^2}{2\beta P_o x^2}\left[\left(\dfrac{\alpha}{\epsilon_f}+\gamma\right)(\sqrt{}-1) - \gamma\left(1-\dfrac{1}{\sqrt{}}\right)\right], & \text{for } 0 < x \leq 1 \\ \qquad \text{with } \sqrt{} = \sqrt{1+\dfrac{4\beta P_o}{(\alpha+\epsilon_f\gamma)^2}} \text{ and } \gamma = \dfrac{1-x}{x} & (34) \\ y = \dfrac{\alpha\epsilon_f}{2\beta P_o}\left(\sqrt{1+\dfrac{4\beta P_o}{\alpha^2}} - 1\right), & \text{for } x = 1 \\ \quad = \dfrac{\epsilon_f}{\epsilon_m}, & \text{for } x = 1 \text{ (as is explained below).} \end{cases}$$

For $x = 1$, equation (31) gives $\sigma = D = 0$, therefore we must conclude from figure 2 that $E_i = -E_c$ for $x = 1$. By (33) this is

$$E_i = -E_c = -\frac{\alpha}{2\beta}\left[\sqrt{1+\frac{4\beta P_o}{\alpha^2}} - 1\right].$$

Again from figure 2 we find

$$\frac{1}{\epsilon_m} = \frac{E_c}{P_o} = \frac{\alpha}{2\beta P_o}\left(\sqrt{1+\frac{4\beta P_o}{\alpha^2}} - 1\right),$$

which leads to $y(1) = \dfrac{\epsilon_f}{\epsilon_m}$.

5 INFLUENCE OF THE EXTERNAL LOAD

In the previous section the mathematical expressions for the normalized current output y(x) have been derived for various conditions. In this section they will be discussed. Where necessary, the following experimental values are introduced:

$$\ell = 0.32 \text{ cm}$$

$$t_o = 0.7 \quad 10^{-6} \text{ sec}$$

$$A = 2.0 \quad \text{cm}^2$$

$$\epsilon_i = 0.886 \quad 10^{-10} \frac{\text{amp} \cdot \text{sec}}{\text{v} \cdot \text{cm}}$$

$$M = \frac{\ell t_o}{\epsilon_i AR} = 1.264 \cdot 10^3 \frac{1}{R}$$

$$T = \frac{Rt_o}{2L} = 3.5 \cdot 10^{-7} \frac{R}{L}$$

$$N = \frac{\ell t_o^2}{\epsilon_i LA} = 0.885 \cdot 10^{-3} \frac{1}{L}$$

$$P_o = 8.06 \quad 10^{-6} \text{ coulombs/cm}^2$$

$$\alpha = 0.886 \cdot 10^{-10} \text{ coulombs/v} \cdot \text{cm}$$

$$\beta = 2.2 \cdot 10^{-14} \text{ coulombs/v}^2$$

Again, as in section 1, we start with the simple assumption (3) rather than (4). The first case to be considered is that of a short circuit R = L = 0:

$$y = \frac{1+S}{(1+Sx)^2} \quad . \tag{10}$$

Here the only parameter is $S = \epsilon_i/\epsilon_f - 1$. Figure 3 shows a set of curves for different S. For S = 0, the current output is constant. Our experiments gave curves of the type S > 0 (i.e. $\epsilon_i > \epsilon_f$) only.

For the case $R \neq 0$, $L = 0$, we have the solution (13) for S = 0 and (16) for $S \neq 0$. Figures 4 and 5 show curves for S = 0 and S = 1, respectively; the parameter R has the values 0, 10, 100, 1000, 10,000, 100,000 ohms. The limiting value R = 0 is described by equation (10). For the other limiting value $R \to \infty$ (for any S) we get

$$y(x) = M (1 + S) x = \frac{\ell t_o}{\epsilon_f AR} x \quad . \tag{35}$$

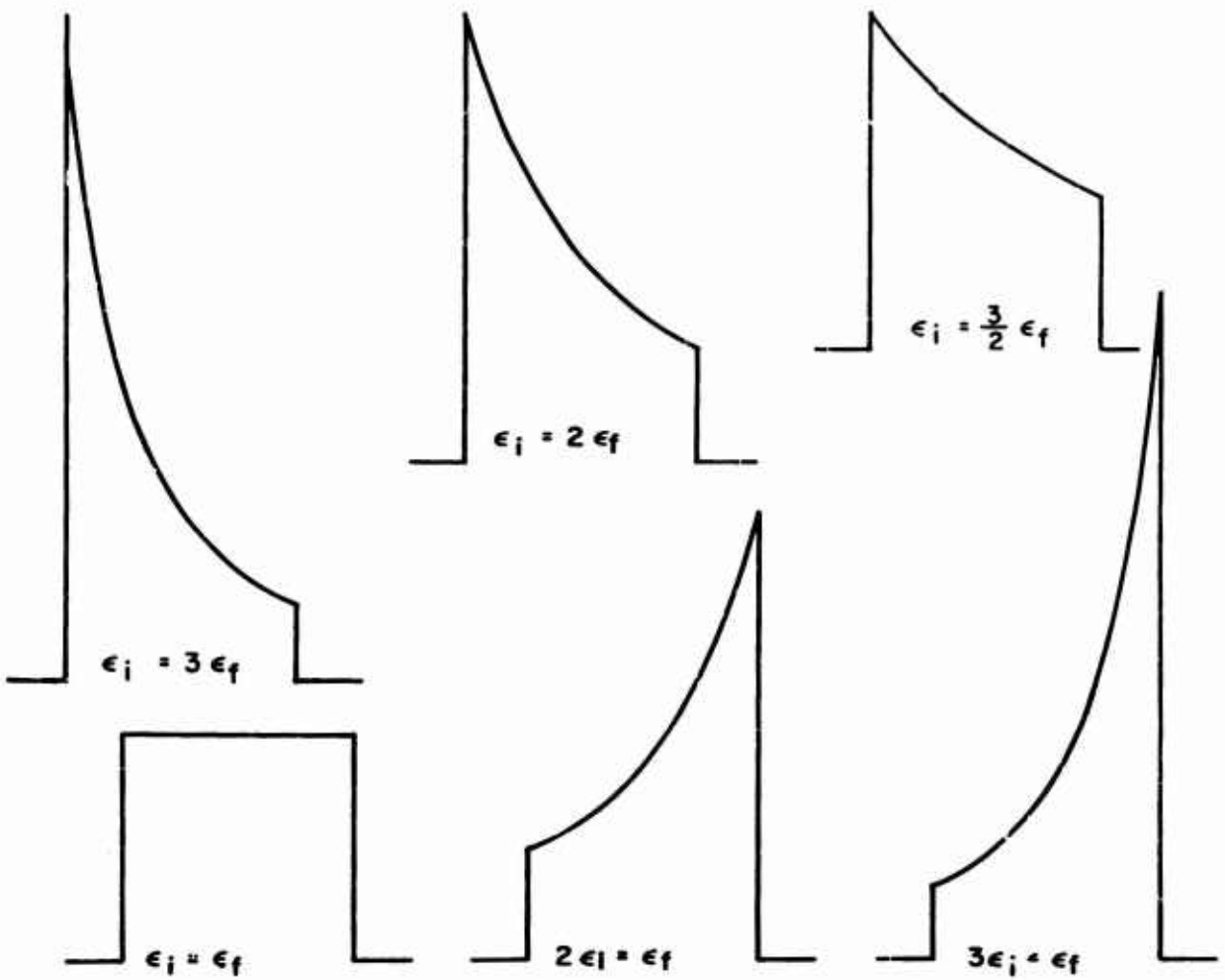

Figure 3. Influence of the ratio ϵ_i/ϵ_f on the curve shape (for short circuit R = L = 0).

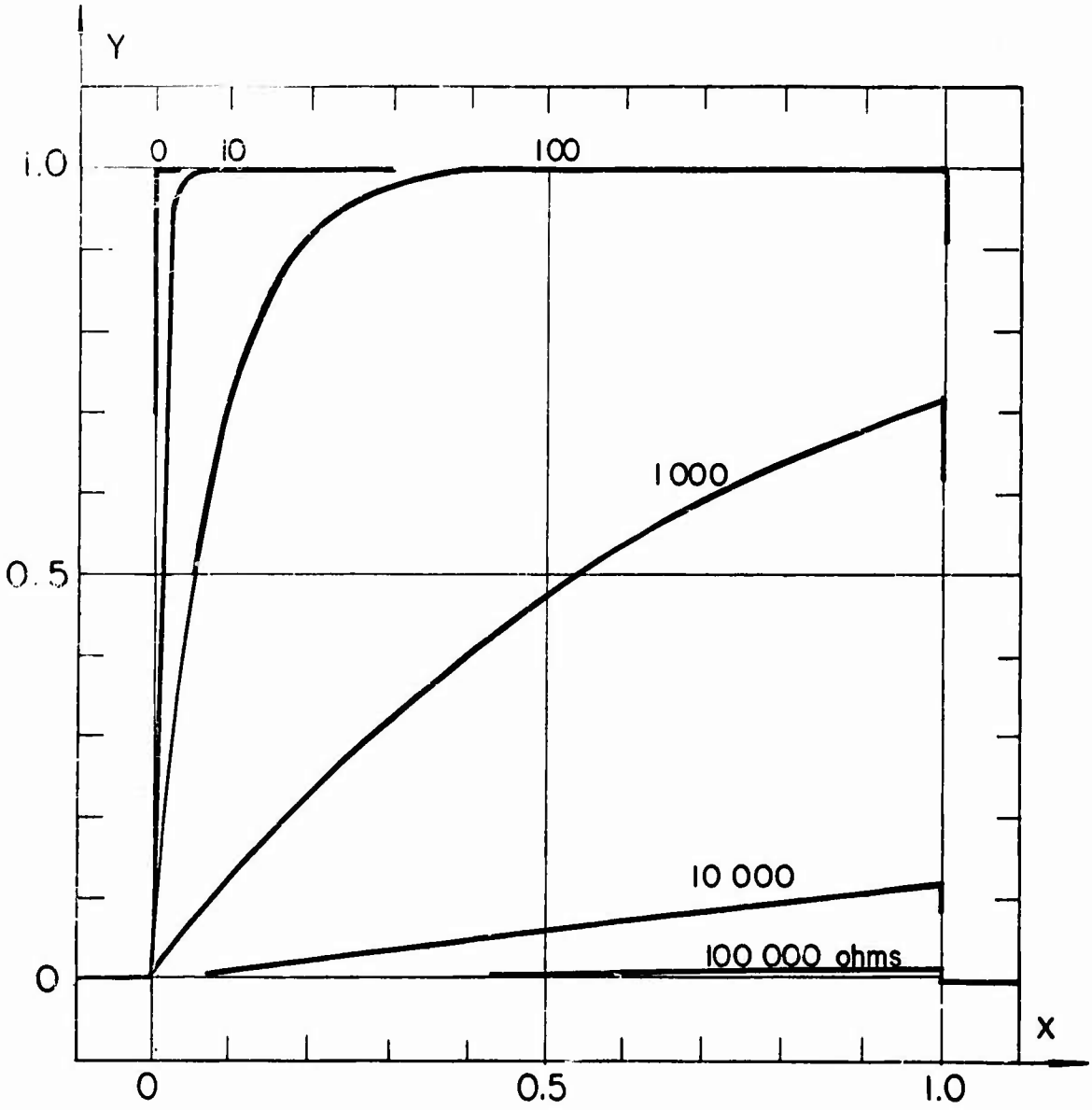

Figure 4. Influence of R on the curve shape (for $\epsilon_i = \epsilon_f$, L = 0)

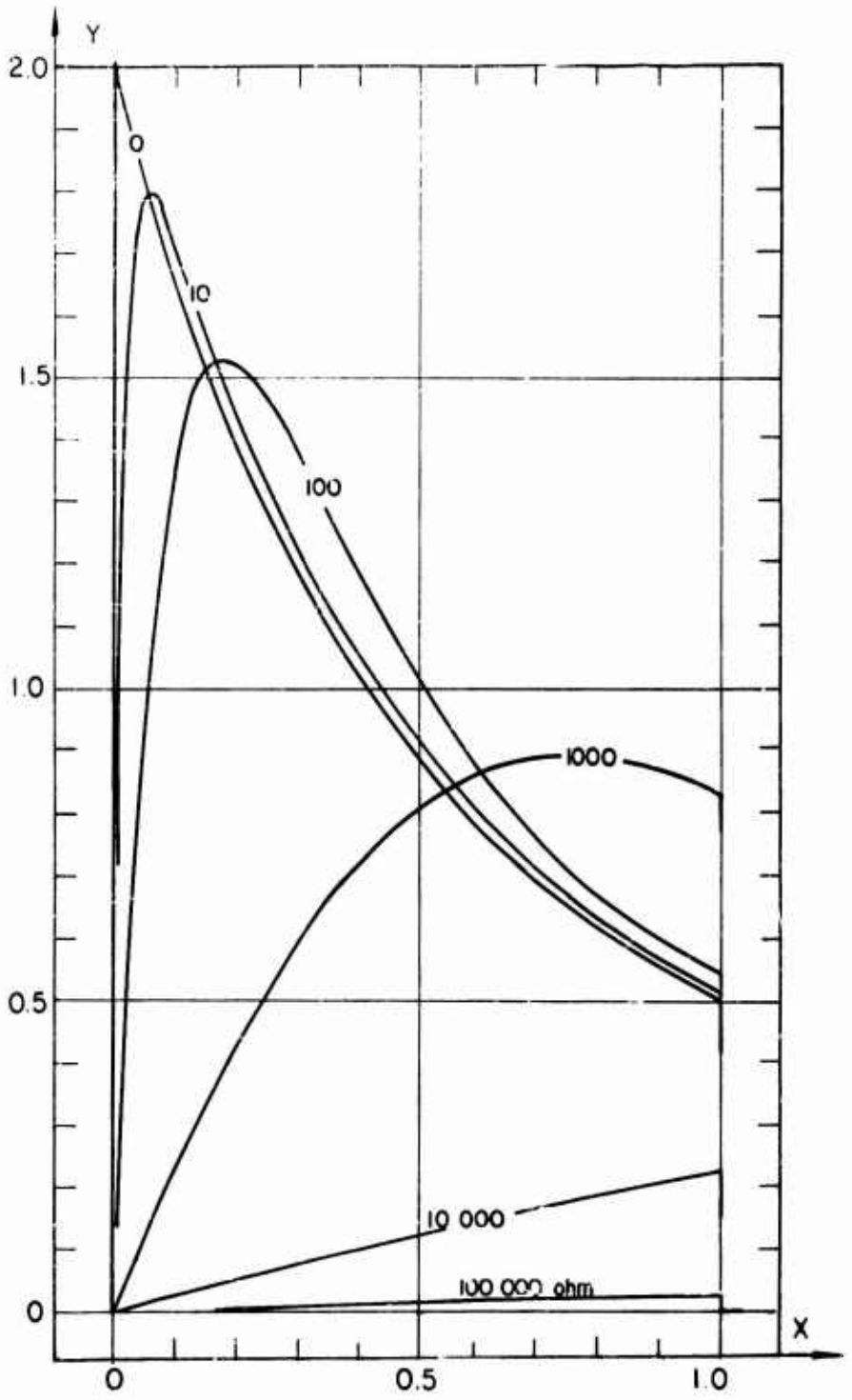

Figure 5. Influence of R on the curve shape (for $\epsilon_1 = 2\epsilon_f$, E = 0)

This means that for an open circuit the curve $y(x)$ for increasing x goes on rising with its initial slope, as given by equation (17). Equation (35) can be found in the following way (using $M = 0$ for $R = \infty$). If $S = 0$, we get from (13) $y = 1 - (1 - Mx) = Mx$. If $S \neq 0$, we take equation (16a), put in $\Gamma = M\left(x + \frac{S}{2}x^2\right) = 0$ and get $y = M(1 + S)x$.

It should be mentioned that the curves of figure 5 could have been plotted using one of the equations (16), a tedious task. DOFL's analog computer was used instead, which employs the differential equation (11) rather than its solution.

The next case to be discussed is that for $R \neq 0$, $L \neq 0$. For R the fixed value 10 ohms is used (which corresponds with the experiments). Figure 6, with $S = 0$, shows a curve for $L = 10^{-7}$ henry and is plotted according to equation (26a). Figure 7, with $S = 1$, shows curves for $L = 0.5 \cdot 10^{-7}$ and $1 \cdot 10^{-7}$ henry. They are plotted by DOFL's analog computer, using the differential equation (24). With all these curves we note oscillations which are damped after one or two periods superimposed on the basic curves for $R = 10$ ohms and $L = 0$. Higher values of L (not shown here) result in oscillations of still higher amplitude and less damping, until eventually the whole curve shape is masked by these oscillations. As far as the experiments are concerned, the inductance is a disturbance and should be as small as possible. The values for L shown in figures 6 and 7 are about those that can be expected. They can influence only the very first part of the pulse.

Introducing the quadratic fit (4) for the hysteresis of the uncompressed material, instead of the linear fit (3) as used hitherto in this section, we discuss the short circuit case $R = L = 0$. In order to point out the difference between (4) and (3), the following results have to be compared with the former results with equation (10) (see fig. 3). The calculation employing the quadratic fit (4) is in better agreement with experiments (ref 2). Using eaution (34), three curves have been calculated and plotted in figures 8, 9, and 10. The values of α, β, P_o (as given in the beginning of this section) were measured statically with elements of the type used in the shock experiments. A dynamic measurement of α and β, imitating the actual shock conditions, is planned. So far, however, no better values are known. As dielectric constants behind the shock front have been assumed: $\epsilon_f = 1250 \cdot \epsilon_o$ (fig. 8), $\epsilon_f = 1540 \cdot \epsilon_o$ (fig. 9), and $\epsilon_f = 2000 \cdot \epsilon_o$ (fig. 10). Using a mean value (according to (3)) of $\epsilon_i = 4400 \cdot \epsilon_o$, this corresponds to $S = 2.5$, 1.9, and 1.2 respectively (see fig. 3 for comparison).

With equation (10) we had the following situation: The curve starts with $y(0) = \epsilon_i/\epsilon_f$ and decreases steadily with increasing x until $y(1) = \epsilon_f/\epsilon_i$. With equation (34) in essence the same thing happens, except that ϵ_i is not a constant (see fig. 2).

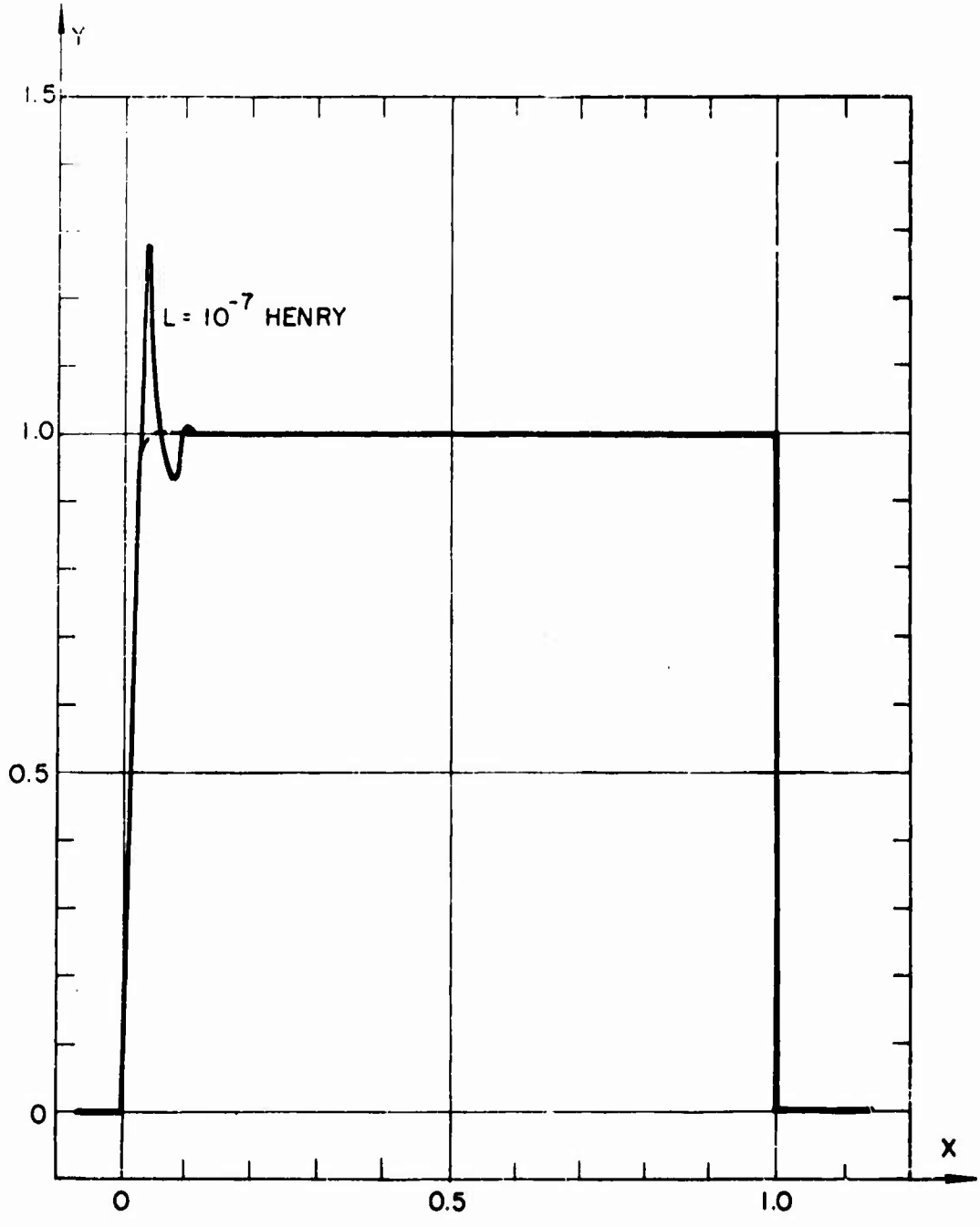

Figure 6. Influence of $L = 10^{-7}$ henry on the curve shape (for $\epsilon_i = \epsilon_f$, R = 10 ohms).

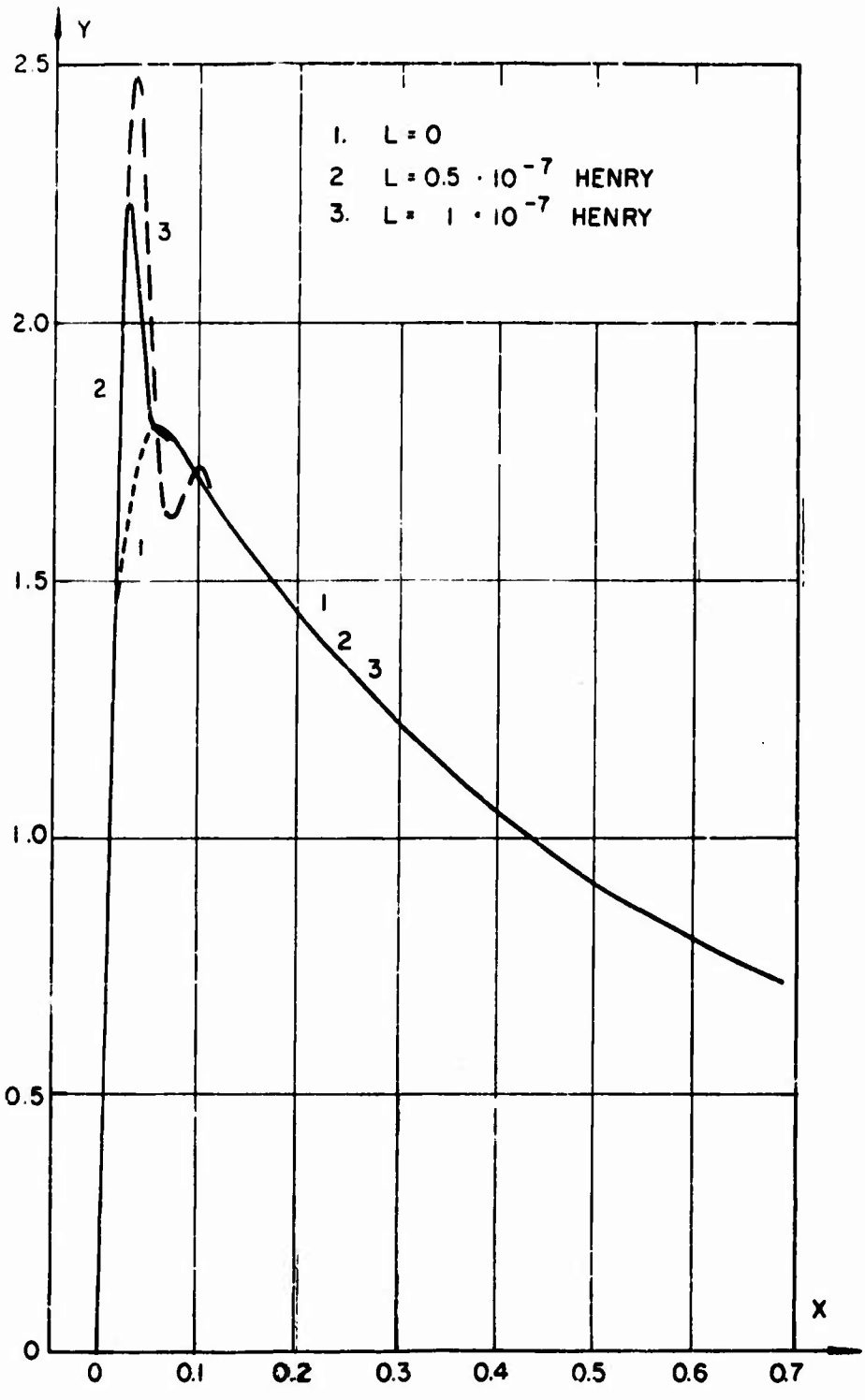

Figure 7. Influence of L = 0.5 and 1.10^{-7} henry on the curve shape (for $\epsilon_i = 2\epsilon_f$, R = 10 ohms).

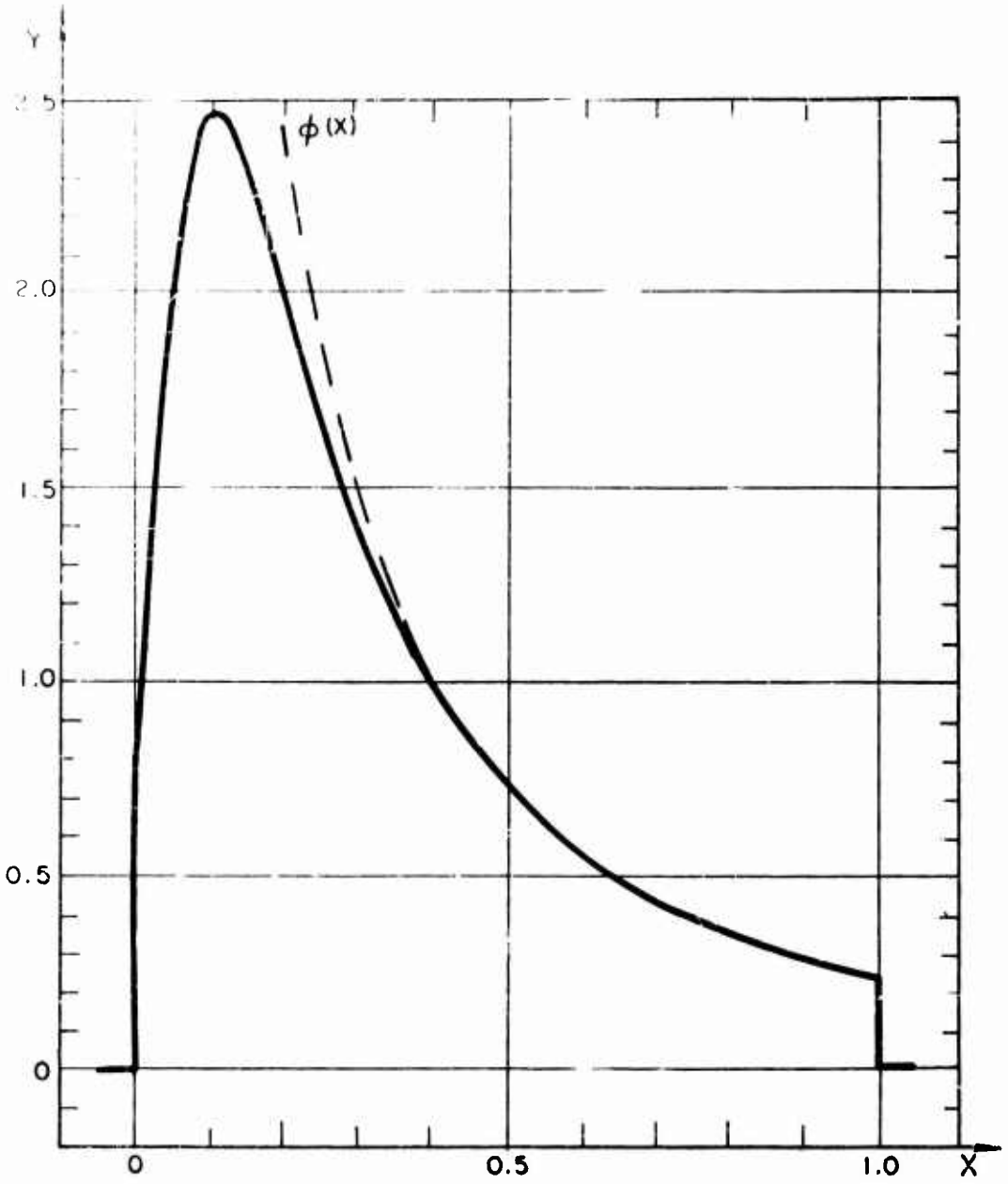

Figure 8. Short circuit current pulse for $\epsilon_f = 1250\ \epsilon_o$ (α, β, P_o as given in section 2 ϕ = auxiliary function)

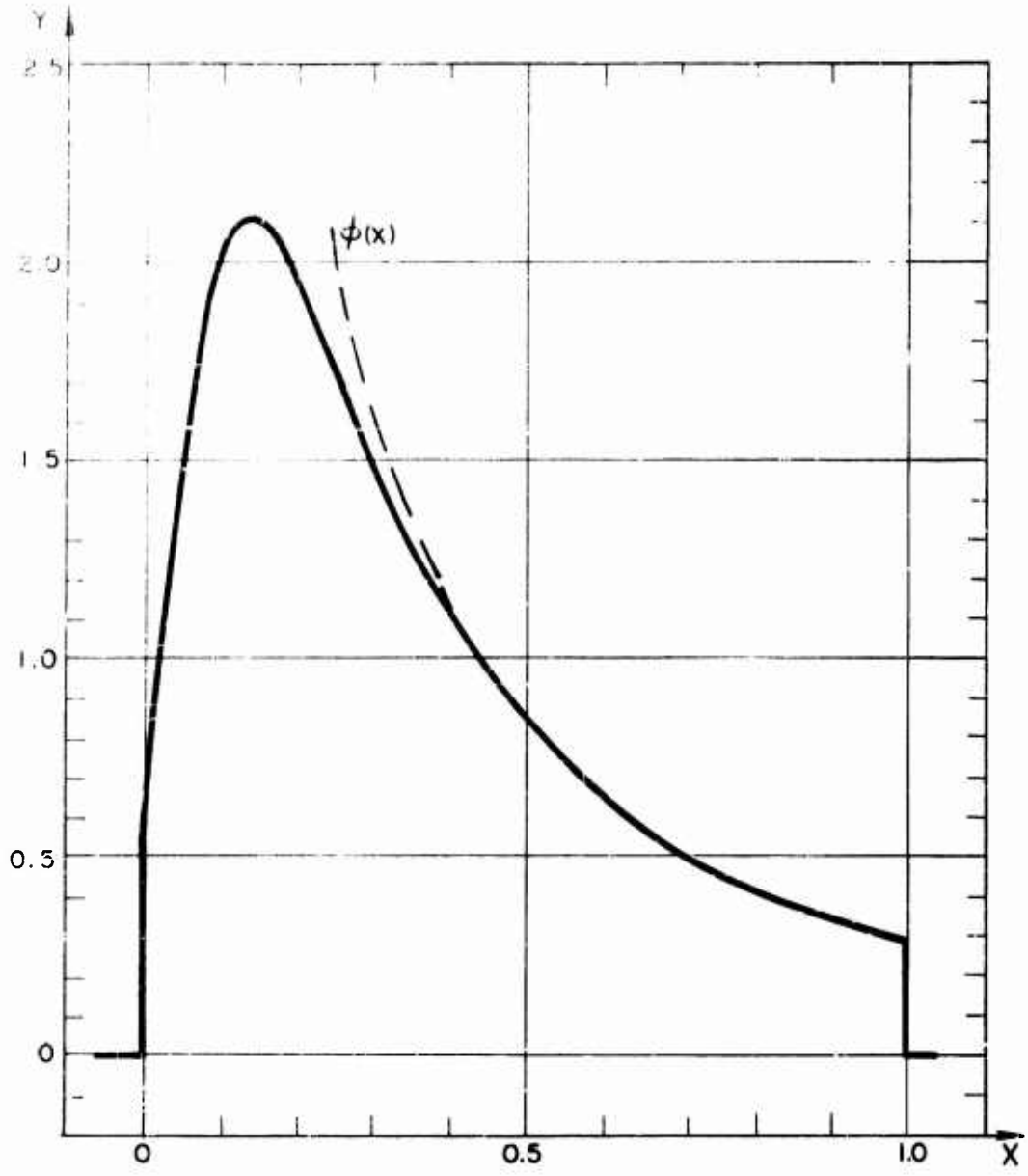

Figure 9. Short circuit current pulse for $\epsilon_f = 1540\ \epsilon_o$ (α, β, P_o as given in section 2; ϕ = auxiliary function).

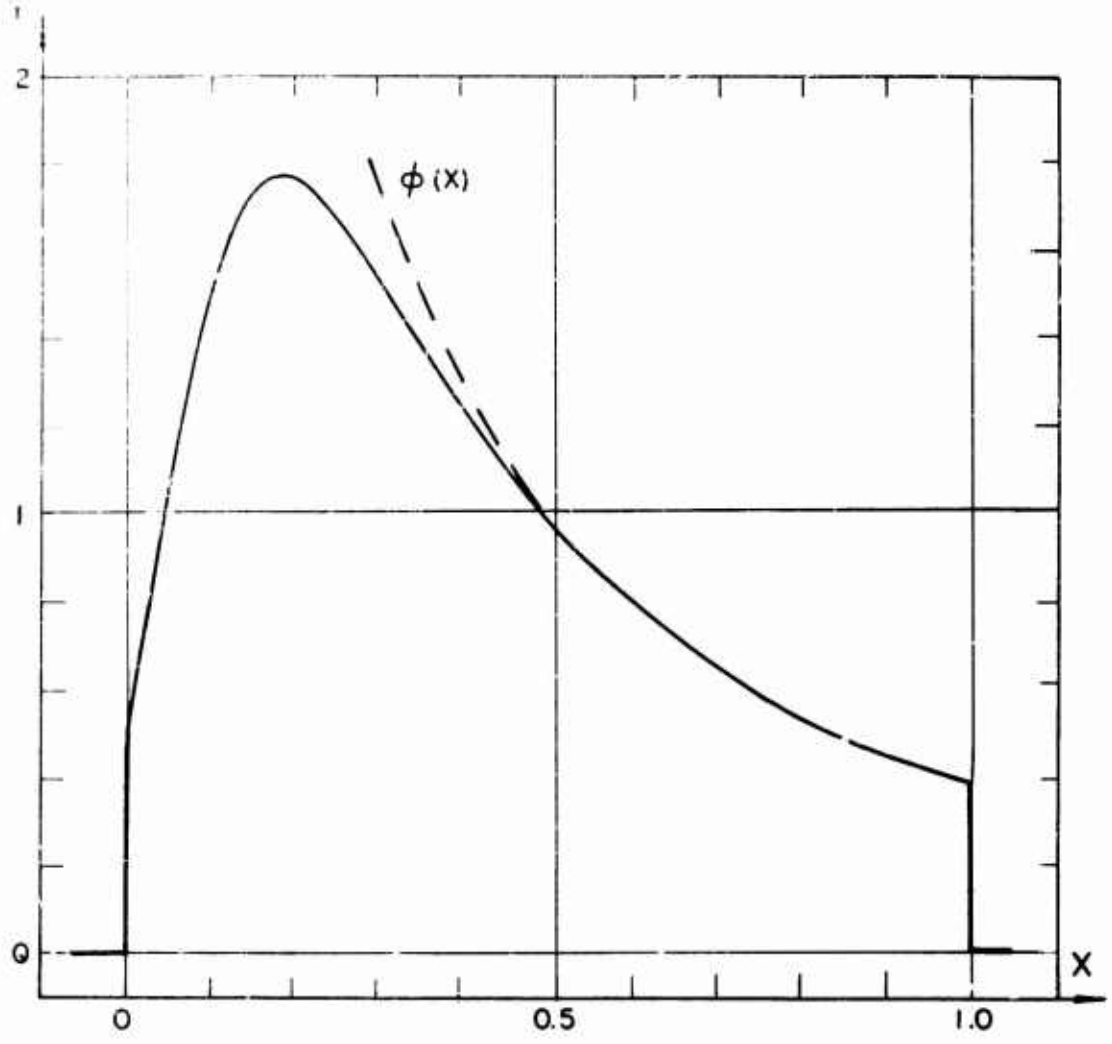

Figure 10. Short circuit current pulse for $\epsilon = 2000\ \epsilon_o$ (α, β, P_o as given in section 2, ϕ = auxiliary function).

Now ϵ_i starts with the value α and ends with the value ϵ_m. Therefore the curve starts with the $y(0) = \alpha/\epsilon_f$ and ends with $y(1) = \epsilon_f/\epsilon_m$. In between the curve shows a maximum. The curve also has a marked bend in its rise, which in some cases could be observed in the experimental results, but in most cases was masked by other effects. The meaning of the auxiliary function $\Phi(x)$ will be explained later.

4. CURRENT-OUTPUT BEYOND $t = t_o$

So far nothing has been said about the current output for $t > t_o$, i.e, for the time after the shock front has reached the back surface of the element. The free charge on the electrodes at the time $x = 1$ ($t = t_o$) is $Q(1)$ and can be calculated from the appropriate equations.

If there is no disturbance by further shock or rarefaction waves or reflections from the side walls, and if the connecting wires do not break, the element then is nothing but a capacitor. It has a uniform (compressed) material with the dielectric constant ϵ_f. Neglecting the slight geometrical compression (shrinkage of ℓ), the capacitance is

$$C = \frac{A\epsilon_f}{\ell} \quad .$$

Remembering $M = \dfrac{\ell t_o}{\epsilon_i AR}$ and $1 + S = \epsilon_i/\epsilon_f$ we find the identity

$$M\,(1 + S) = \frac{t_o}{RC} \quad ,$$

which is the normalized decay time of the element as a capacitor. For the time $x > 1$ this capacitor discharges according to the law

$$Q(x) = Q(1) \cdot e^{-M(1 + S)\,(x - 1)} . \tag{36}$$

With $y = -\dfrac{1}{Q_o}\dfrac{dQ}{dx}$ the normalized discharging current is

$$y = \frac{Q(1)}{Q_o} M(1+S) \cdot e^{-M(1 + S)\cdot(x - 1)} \quad \text{for } x > 1 \tag{37}$$

The total charge output is

$$\int_0^{\infty} y\,dx = -\frac{1}{Q_o}\int_0^{\infty}\frac{dQ}{dx}\,dx = -\frac{1}{Q_o}\int_{Q_o}^{0} dQ = 1 \tag{38}$$

which is equivalent to

$$\int_0^{\infty} I\,dt = Q_o \cdot \tag{39}$$

For case R = 0, L = 0, any S, we get from equation (9) or (31)

$$Q(1) = 0 \tag{40}$$

$$Q(x) = y(x) = 0 \qquad \text{for } x > 1 \tag{41}$$

$$\int_0^1 y \, dx = 1. \tag{42}$$

This result is typical for a short circuit, it is independent of S and the assumption about the hysteresis curve.

For case $R \neq 0$, L = 0, S = 0, we get from equation (12)

$$Q(1) = \frac{Q_o}{M} (1 - e^{-M}) \tag{43}$$

and

$$Q(x) = \frac{Q_o}{M} (1 - e^{-M}) e^{-M(x-1)} \tag{44}$$

$$y(x) = (1 - e^{-M}) e^{-M(x-1)} \qquad \text{for } x > 1. \tag{45}$$

For case $R \neq 0$, L = 0, $S \neq 0$, we get from equation (15)

$$Q(1) = Q_o e^{-M(1+\frac{S}{2})} \left[1 + M\int_0^1 (1 - z) e^{M(z + \frac{S}{2} z^2)} dz\right] \tag{46}$$

and

$$Q(x) = Q_o e^{\frac{MS}{2}} [\ldots\ldots] e^{-M(1+S)x} \tag{47}$$

$$y(x) = M(1 + S) e^{\frac{MS}{2}} [\ldots\ldots] e^{-M(1+S)x} \qquad \text{for } x > 1. \tag{48}$$

For case R = 0, $L \neq 0$, S = 0, we get from equation (21)

$$Q(1) = \frac{Q_o}{\sqrt{N}} \sin\sqrt{N} \quad , \quad \text{with } N = \frac{\ell t_o^2}{\theta_i \mu A} \tag{49}$$

and

$$Q(x) = \frac{Q_o}{\sqrt{N}} (\sin\sqrt{N}) e^{-M(x-1)} \tag{50}$$

$$y(x) = \frac{M}{\sqrt{N}} (\sin\sqrt{N}) e^{-M(x-1)} \qquad \text{for } x > 1. \tag{51}$$

The case $R \neq 0$, $L \neq 0$, S = 0, can be handled in the same manner, using equation (25).

5. MAXIMUM ENERGY OUTPUT

For some applications the question arises as to which value of R results in a maximum of energy output, W.

$$W = \int_0^{T} I^2 \cdot R \, dt. \tag{52}$$

this problem can be calculated analytically for the case S = 0. The definition of the effective pulse length T is somewhat arbitrary, and depends on the experimental conditions. We put $T = t_o$, because the experiments indicate that the discharge virtually comes to an end at t_o, due to rarefaction waves and subsequent breaking of the wires. It must be noted that in general not all the free charge from the element can flow off during this time.

We limit the calculation to the case $R \neq 0$, $L = 0$, $S = 0$, with the current output

$$y = 1 - e^{-Mx} \qquad \text{with} \quad M = \frac{\ell t_o}{\epsilon_i A R} \tag{13}$$

$$x = \frac{t}{t_o}$$

from which follows

$$I(t) = -\frac{Q_o}{t_o} y = -\frac{Q_o}{t_o}\left(1 - e^{-\frac{M}{t_o}t}\right) \tag{53}$$

$$W = \int_0^{t_o} I^2 R \, dt \tag{52}$$

$$W = \frac{Q_o^2 \ell}{\epsilon_i A}\left[\frac{1}{M} - \frac{3}{2M^2} + \frac{2}{M^2} e^{-M} - \frac{1}{2M^2} e^{-2M}\right] . \tag{54}$$

W becomes a maximum for a certain value of R or M, which is determined by putting $\frac{dW}{dM} = 0$. This leads to the equation

$$3 - M - (4 + 2M)\, e^{-M} + (1+M)\, e^{-2M} = 0$$

with the solution $M = 1.8926$. With this value the maximum energy output is, according to (54)

$$W_{max} = \frac{Q_o^2 \ell}{\epsilon_i A} \cdot 0.19 \tag{55}$$

This is only 38 percent of the potential energy of the element, if it is considered a capacitor of capacitance

$$C = \frac{A\epsilon_i}{\ell}$$

which has the potential energy

$$W = \frac{Q_o^2}{2C} = \frac{Q_o^2 \ell}{\epsilon_i A} \cdot 0.5 \quad .$$

The total charge output up to the time t_o is according to equation (43)

$$Q_o - Q(1) = Q_o\left(1 - \frac{1}{M} + \frac{1}{M} e^{-M}\right) = Q_o \cdot 0.55 \quad . \tag{56}$$

Using the specific values from our experiments as introduced in section 2, we get $M = \frac{1264}{R}$ which in combination with $M = 1.8926$ leads to

$$R = 668 \text{ ohms}$$

as the value of the external resistor for which the energy output is a maximum. The latter is according to (55)

$$W_{max} = 8.9 \cdot 10^{-2} \text{ joules.}$$

6. CONDUCTIVITY BEHIND THE SHOCK FRONT

So far the assumption has been made that a ferroelectric material is nonconducting behind as well as in front of the shock front, at least for a pressure below 125 kilobar and temperatures below 150°C. However, there is at least one reference in the literature (ref 3) stating a specific resistivity $\rho = 1000$ ohm · cm for a pressure of 300 kilobar in barium titanate. As the following calculations will show, a resistivity larger than $\rho = 10^5$ ohm · cm should not be detectable in the output curves (in a short-circuit situation), and may therefore be regarded as infinite. The influence of a lower resistivity is the topic of the following calculations. The model used in section 2 (fig. 1) is introduced again, with $L = 0$ and R very small (short-circuit assumption). The linear fit to the hysteresis curve, equation (3), is used. The conductivity behind the shock front is treated as a shunt resistor with the resistance

$$r = \rho \frac{\xi}{A} = \rho \frac{\ell t}{A t_o} \quad ,$$

ρ is the specific resistivity of the material under compression.

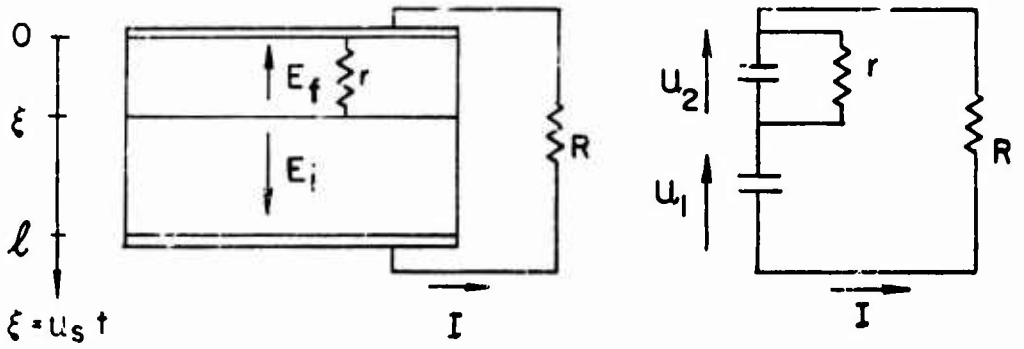

Figure 11. Element as the shock front travels through it, and equivalent circuit.

In the former treatment (section 2) it was supposed that no free charge can accumulate at the interface between the two regions of the element (in other words: at the shock front), which is equivalent to the statement that the dielectric displacement D (equal to the charge density σ) is continuous through this interface.

Now we have a shunt resistor which draws a certain current i, therefore D is different in each region of the element. D_i is σ in the region before the shock front. Behind it, D_f is $\overline{\sigma}$ which is smaller than σ.

The basic equation is $U_1 + U_2 + U_3 = 0$, or with short-circuit assumption $U_1 + U_2 = 0$. We look at the regions of the element as capacitors, with capacitance

$$C = \frac{Q}{U} = \frac{DA}{U} = \frac{\epsilon A}{d}$$

It follows

$$U = \frac{D}{\epsilon} d$$

$$U_i = \frac{\sigma - P_o}{\epsilon_i} (\ell - \xi) = \frac{\sigma - P_o}{\epsilon_i} \frac{\ell}{t_o} (t_o - t)$$

$$U_2 = \frac{\overline{\sigma}}{\epsilon_f} \xi = \frac{\overline{\sigma}}{\epsilon_f} \frac{\ell}{t_o} t$$

and also

$$U_2 = i \cdot r = i \frac{\rho \ell t}{A t_o}$$

The displacement current is

across the front region $I = A \frac{dc}{dt}$ and

across the back region $I-i = A \frac{d\bar{\sigma}}{dt}$,

from which it follows that

$$i = A \left(\frac{d\sigma}{dt} - \frac{d\bar{\sigma}}{dt}\right) . \tag{57}$$

The two expressions for U_2 combined result in a differential equation for $\dot{\sigma}$:

$$\frac{d\bar{\sigma}}{dt} + \frac{1}{\rho \epsilon_f} \bar{\sigma} = \frac{d\sigma}{dt} ,$$

whose solution through the initial value $\bar{\sigma} = \sigma$ for $t = 0$ is

$$\sigma = \sigma - \frac{1}{\rho \epsilon_f} e^{-\frac{t}{\rho \epsilon_f}} \int_0^t \sigma \, e^{\frac{t}{\rho \epsilon_f}} dt \tag{58}$$

and can be used to eliminate $\bar{\sigma}$.

Introduction of this $\bar{\sigma}$ into any of the two equations for U_2 leads to

$$U_2 = \frac{\ell \sigma t}{\epsilon_f t_o} - \frac{\ell t}{\epsilon_f^2 \rho t_o} e^{-\frac{t}{\rho \epsilon_f}} \int_0^t \sigma \, e^{\frac{t}{\rho \epsilon_f}} dt.$$

Now the basic equation is

$$U_1 + U_2 = \frac{\sigma - P_o}{\epsilon_i} \frac{\ell}{t_o} (t_o - t) + \frac{\sigma}{\epsilon_f} \frac{\ell}{t_o} t - \frac{\ell}{\epsilon_f^2 \rho} \frac{t}{t_o} e^{-\frac{t}{\rho \epsilon_f}} \int_0^t \sigma e^{\frac{t}{\rho \epsilon_f}} dt = 0 \tag{59}$$

which must be solved for $\sigma(t)$. It may be noted, by comparison with equation (1), that the third term only expresses the disturbance due to a finite value of ρ and disappears with $\rho \to \infty$.

Again as in section 1, the following expressions are introduced:

$x = t/t_o$

$S = \epsilon_i/\epsilon_f - 1$

$Q = A \sigma$

$Q_o = A P_o$, and furthermore

$\eta = \frac{t_o}{\epsilon_f \rho} = \frac{t_o(1+S)}{\epsilon_i \rho}$

This gives

$$Q(1 + Sx) - Q_o(1 - x) - A\frac{\epsilon_i}{\epsilon_f}\eta x\, e^{-\eta x}\int_0^x \sigma e^{\eta x}\, dx = 0 \qquad (60)$$

which for $\rho \to \infty$ ($\eta \to 0$) approaches equation (8).

Now the integral equation is transformed into a differential equation by dividing it by $x\, e^{-\eta x}$, differentiating it with respect to x, and multiplying it by $x^2\, e^{-\eta x}$, which results in

$$\frac{dQ}{dx}(x + Sx^2) - (Q - Q_o)(1 - \eta x + \eta x^2) = 0. \qquad (61)$$

Since Q(x) and $\frac{dQ}{dx}$ must approach the formulas (9) and (10) for x = 0 (because in the beginning the shunt resistor is r = 0), we have the following initial conditions:

$$Q = Q_o, \text{ and } \frac{dQ}{dx} = -Q_o(1 + S) \quad \text{for } x = 0 .$$

From the proper solution Q(x), the normalized current y(x) is derived as prescribed by equation (6). Skipping some intermediate calculations, the final solutions to equation (61) are:

for S = 0

$$Q = Q_o\left[1 - x\, e^{-\eta x(1 - \frac{x}{2})}\right] \qquad (62a)$$

$$y = (1 - \eta x + \eta x^2)\, e^{-\eta x(1 - \frac{x}{2})} , \qquad (63a)$$

for S ≠ 0

$$Q = Q_o\left[1 - (1 + S)\, x\, e^{\frac{\eta}{S}x}(1 + Sx)^{-\frac{S^2+\eta+\eta S}{S^2}}\right] \qquad (62b)$$

$$y = (1 + S)(1 - \eta x + \eta x^2)\, e^{\frac{\eta}{S}x}(1 + Sx)^{-\frac{2S^2+\eta+\eta S}{S^2}} \qquad (63b)$$

For $\rho \to \infty$ ($\eta \to 0$), these equations approach the former ones, namely

(62a), (62b) → (9)

(63a), (63b) → (10) .

The total charge output within the normal pulse length x = 1 is $Q_o - Q(1)$, or relative to the maximum output Q_o :

$$\frac{Q_o - Q(1)}{Q_o} = e^{-\frac{\eta}{2}} \qquad \text{for } S = 0$$

$$\frac{Q_o - Q(1)}{Q_o} = e^{+\frac{\eta}{S}(1+S) - \frac{\eta+\eta S}{S^2}} \qquad \text{for } S \neq 0$$

Using $\eta = \dfrac{t_o(1+S)}{\epsilon_i \rho}$, this is

$$\frac{Q_o - Q(1)}{Q_o} = e^{-\frac{t_o}{2\epsilon_i \rho}} \qquad \text{for } S = 0 \qquad (64a)$$

$$\frac{Q_o - Q(1)}{Q_o} = e^{-\frac{t_o(1+S)}{\epsilon_i S \rho}(1+S) - \frac{t_o(1+S)^2}{\epsilon_i S^2 \rho}} \qquad \text{for } S \neq 0 \qquad (64b)$$

Examples are calculated for $S = 0$ ($\epsilon_i = \epsilon_f$), $S = 1$ ($\epsilon_i = 2\epsilon_f$), and $S = 2$($\epsilon_i = 3\epsilon_f$). Since the calculated values depend on the assumption about ϵ_i, the dielectric constant in the uncompressed material, its two limiting values (see fig. 2) $\epsilon_i = \alpha = 1000\ \epsilon_o$ (for small field) and $\epsilon_i = \epsilon_m = 5000\ \epsilon_o$ (for maximum field)are both used, the correct value lies in between α and ϵ_m. The results are shown in the following table. In most cases, the values based on $\epsilon_i = \alpha$ or $\epsilon_i = \epsilon_m$ are approximately the same for a given ρ, also the influence of S is small. In general, the charge output is higher than 95 percent if $\rho > 10^5$ ohm cm, and higher than 90 percent if $\rho > 3 \cdot 10^4$ ohm cm*.

Figures 12 and 13 show some curves of the normalized current output y(x) calculated for certain values of ρ. Figure 12 shows the case $\epsilon_i = \epsilon_f$, according to equation (63a), figure 13 the case $\epsilon_i = 2\epsilon_f$, according to equation (63b).

7. CURRENT OUTPUT UNDER AN OBLIQUE IMPACT

In an actual experiment the projectile may hit the element with a larger or smaller angle of impact. In this section the deformation of

---

* Recent experiments with barium titanate ceramic (ref 2) gave values $\frac{Q_o - Q(1)}{Q_o} = 91 \pm 5\ \%$ for 110 kilobar, thus indicating a resistivity of 10^5 ohm cm.

Table 1. Charge Output in Percent of the Initial Charge, if There is a Resistivity ρ Behind the Shock Front (for Short Circuit R = L = 0).

ρ ohm cm	relative charge output $\frac{Q_o - Q(1)}{Q_o}$ in percent for					
	$\epsilon_i = \epsilon_f$		$\epsilon_i = 2\epsilon_f$		$\epsilon_i = 3\epsilon_f$	
	$\epsilon_i = \alpha$	$= \epsilon_m$	$= \alpha$	$= \epsilon_m$	$= \alpha$	$= \epsilon_m$
10^7	100.0	100.0	100.0	100.0	99.9	100.0
$3 \cdot 10^6$	99.9	100.0	99.9	100.0	99.7	99.9
10^6	99.6	99.9	99.7	99.9	99.2	99.8
$3 \cdot 10^5$	98.7	99.7	99.0	99.6	97.5	99.5
10^5	96.1	99.2	97.0	98.8	92.6	98.5
$3 \cdot 10^4$	87.7	97.4	90.3	96.0	77.4	95.0
10^4	67.4	92.4	73.7	88.5	46.4	85.6
$3 \cdot 10^3$	26.7	76.8	36.2	66.2	7.7	59.9
10^3	1.9	45.4	4.2	29.5	0.1	21.5
$3 \cdot 10^2$	—	7.2	—	1.7	—	0.6

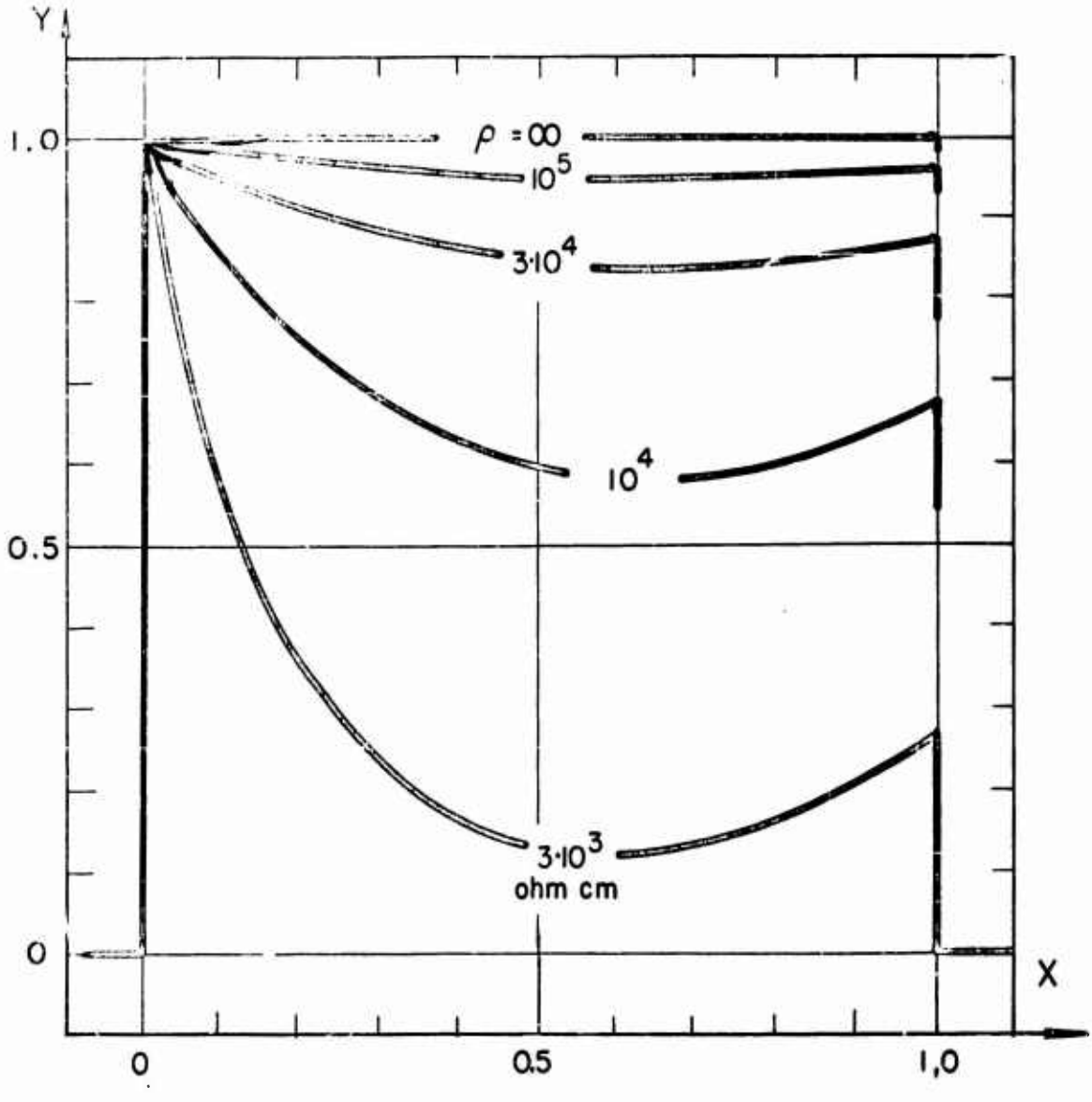

Figure 12. Current pulse with a resistivity ρ in the compressed material ($\sigma_i - \sigma_f$, R = L = 0).

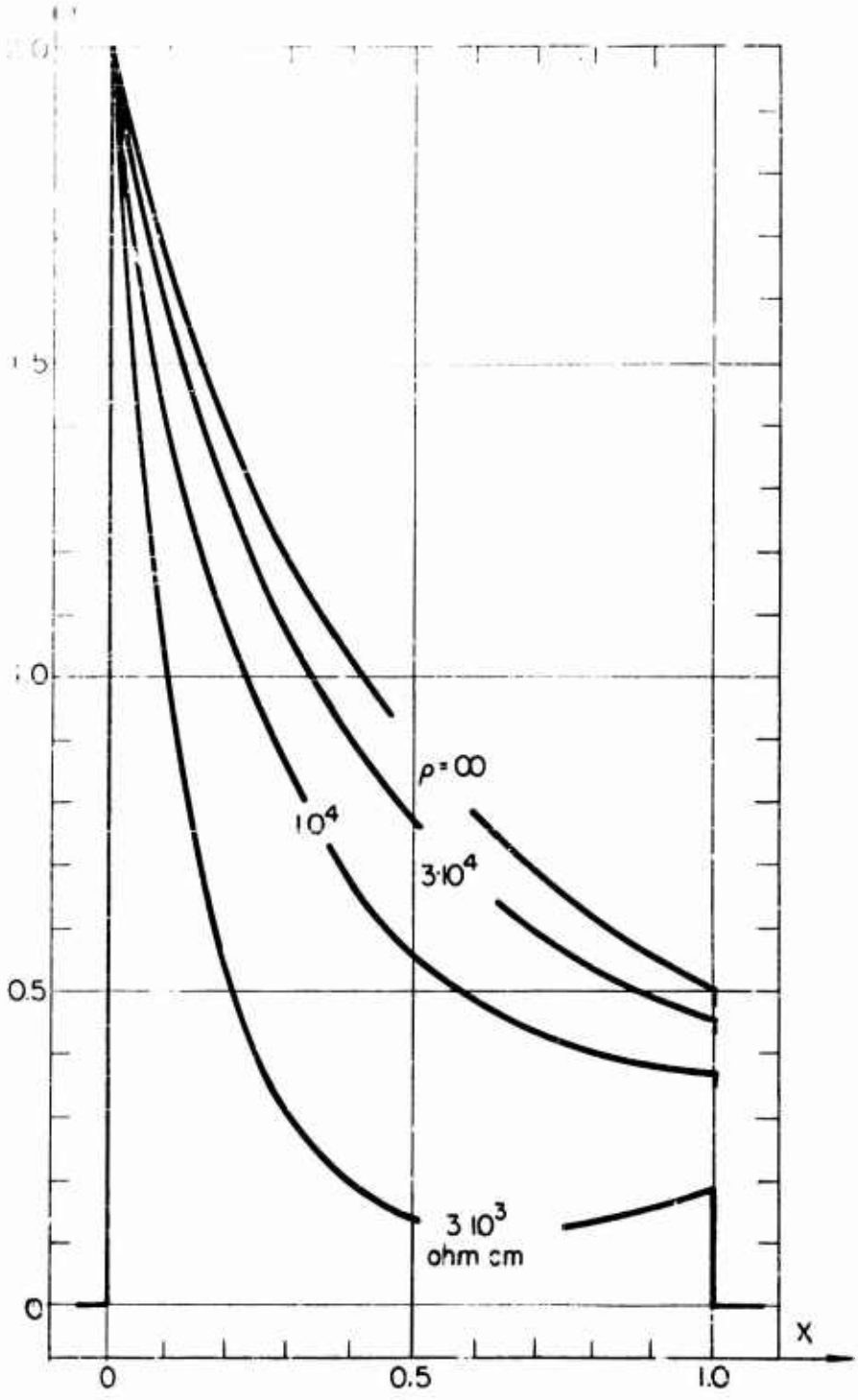

Figure 13. Current pulse with a resistivity ρ in the compressed material ($\epsilon_i = 2\epsilon_f$, R = L = 0).

the pulse due to this angle will be calculated. The short-circuit assumption (R = L = 0) and the linear fit to the hysteresis curve (equation (3)) are used.

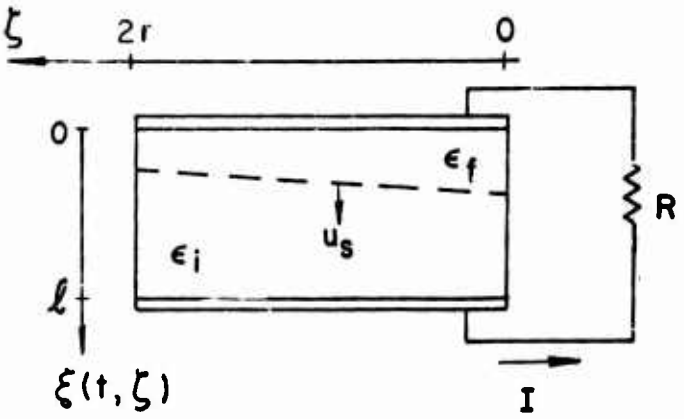

Figure 14. Oblique shock front through the element (angle of shock front exaggerated).

The shock front originates at the edge of the element that is hit first, and the time is counted from that moment on. The back surface of the element along that edge is reached at the time $t_o = \ell/u_s$, again called the "normal pulse length." Other regions of the element experience the shock front with a time delay, the opposite edge has the maximum delay t_a; along that edge the shock front reaches the back surface at the time $t_o + t_a$. The time delay t_a is connected with the angle of impact φ by the formula

$$t_a = \frac{2r}{v} \tan \varphi, \tag{65}$$

with 2r = diameter of the element and v = impact velocity of the projectile. For example with 2r = 5/8 in. and v = 1400 ft/sec, an angle of impact as small as 1/4 deg results in a time delay $t_a = 0.16$ μsec, which must be compared with $t_o = 0.70$ μsec. The angle of the shock front in the material with respect to the planes of the electrodes is about 2.5 deg in this example, since u_s is about 15,000 ft/sec.

In order to start the calculation, the element is thought to be split into small elements, each with the area $dA(\zeta)$ and the thickness ℓ. Each element undergoes the same transition as the shock front travels through it, delayed in time however as we go from one edge to the other.

An oblique shock front results, the angle is assumed sufficiently small (e.g., 2.5 deg, as stated above) so that no correction is needed for the fact that the direction of travel and the normal to the shock front are not in parallel. Besides being the simplest possible formula, the short-circuit assumption is also very convenient here since it requires that the voltage drop across the electrodes be zero. All small elements can therefore be treated as independent elements. The following calculations are confined to the case $t_a \leq t_o$. The current output pulse consists of three parts. The rise time (A) from $t = 0$ to $t = t_a$ is the time during which only a part (increasing with time) of the front electrode is in contact with the projectile and therefore only a part of the element is involved. During the main pulse (B) from t_a to t_o both electrodes are fully involved. The decay time (C) of the pulse from t_o to $t_o + t_a$ is explained by the situation that the back surface has been reached by the shock front and only a decreasing area of the back electrode is producing free charge. It is supposed that reflections from the back end of the element or from the supporting rod do not disturb the process. The calculation starts with a combination of equations (1), (2), and (3):

$$\frac{\sigma - p_o}{\epsilon_1} (\ell - \xi) + \frac{\sigma}{\epsilon_f} \xi = 0. \tag{66}$$

The distance ξ of the shock front from the front electrode (fig. 14) now depends on time t and position ζ:

$$\xi = u_s\left(t - \frac{\zeta}{2r} t_a\right), \quad \frac{\partial \xi}{\partial t} = u_s. \tag{67}$$

All variables are now functions both of t and ζ. The solution of equation (66) must be integrated across the appropriate surface elements $dA(\zeta)$, which gives the charge $Q(t)$.

If the surface of each electrode is a circular area, we have

$$dA(\zeta) = 2\sqrt{2r\zeta - \zeta^2}\, d\zeta, \quad \int_{\zeta=0}^{\zeta=2r} dA = \pi r^2 = A, \tag{68}$$

and the current is

$$I(t) = \int \frac{\partial \sigma(t,\zeta)}{\partial t} dA. \tag{69}$$

The usual transformations are introduced:

$$u_s = \ell/t_o$$

$$S = \epsilon_i/\epsilon_f - 1$$

$$x = t/t_o$$

$$y(x) = -\frac{t_o}{Q_o} \cdot I(x) = -\frac{t_o}{AP_o} I(x)$$

and furthermore

$$z = t_a/t_o = \text{normalized delay time.}$$

It follows

$$\xi = \zeta(x - \frac{\zeta}{2r} z) \quad \text{and from (66)}$$

$$\sigma = P_o \frac{1 - (x - \frac{\zeta}{2r} z)}{1 + S(x - \frac{\zeta}{2r} z)} \quad \text{and from this}$$

$$\frac{\partial \sigma}{\partial t} = - \frac{P_o}{t_o} (1 + S) \frac{1}{(1 + Sx - S\frac{\zeta}{2r} z)^2} .$$

The total normalized current is, with (69)

$$y(x) = \frac{2(1+S)}{A} \int \frac{\sqrt{2r\zeta - \zeta^2}}{(1+Sx-S\frac{\zeta}{2r}z)^2} \, d\zeta . \tag{70}$$

For $z = 0$ equation (70) reduces to equation (10).

For $S = 0$ equation (70) has the form

$$y(x) = \frac{2}{\pi r^2} \int \sqrt{2r\zeta - \zeta^2} \, d\zeta$$

with the solution

$$y(x) = \frac{\zeta - r}{\pi r^2} \sqrt{2r\zeta - \zeta^2} + \frac{1}{\pi} \sin^{-1} (\frac{\zeta - r}{r}) . \tag{71}$$

For $S \neq 0$ equation 70 has the form

$$y(x) = \frac{8(1+S)}{\pi S^2 z^2} \int \frac{\sqrt{2r\zeta - \zeta^2}}{(B - \zeta)^2} \, d\zeta \tag{72}$$

with

$$B = B(x) = \frac{2r}{z} (\frac{1}{S} + x), \text{ which is independent of } \zeta .$$

Here the solution can be found after these transformations

$$B = \zeta - x, \quad d\zeta = -dx$$

$$2r\zeta - \zeta^2 = a + bx - x^2$$

$$a = B(2r-B)$$

$$b = 2(B-r)$$

The solutions of the intergral are different for $a > 0$, $a = 0$, and $a < 0$. Our calculations are confined to $a < 0$, which is equivalent to

$$x > z - \frac{1}{S} \quad .$$

Since actually S falls between 1 and 2, this condition is always fulfilled for $z < 0.5$. For $z \geq 0.5$, the very first part of the pulse may require a different solution. Here we proceed with $a < 0$.

The general solution of the integral in equation (72) is

$$\int \ldots d\zeta = \frac{\sqrt{2r\zeta - \zeta^2}}{B-\zeta} - T \sin^{-1}\left[1 - \frac{\zeta}{r}\left(1 - \frac{2r-\zeta}{B-\zeta}\right) + \sin^{-1}\left(1 - \frac{\zeta}{r}\right)\right] \tag{73}$$

with the abbreviation

$$T = \frac{B-r}{\sqrt{B(B-2r)}} = \frac{1+Sx-Sz/2}{\sqrt{(1+Sx)(1+Sx-Sz)}} \quad . \tag{74}$$

To complete the solutions (71) or (73), the limits of the integrals $\int_{\zeta_1}^{\zeta_2}$ are to be put in. These limits depend on the region of the pulse, as explained above in this section.

Region A (rise time, $0 \leq t \leq t_a$, $0 \leq x \leq z$): for a fixed time t (or x) within this region, the front electrode is covered by the projectile between $\zeta_1 = 0$ and $\zeta_2 = \frac{2r}{t_a} t = \frac{2r}{z} x$.

Region B (main pulse, $t_a \leq t \leq t_o$, $z \leq x \leq 1$): both electrodes are fully involved, so $\zeta_1 = 0$ and $\zeta_2 = 2r$.

Region C (decay time, $t_o \leq t \leq t_o + t_a$, $1 \leq x \leq 1 + z$): the back electrode is only partly involved, therefore

$$\zeta_1 = \frac{2r}{t_a}(t - t_o) = \frac{2r}{z}(x - 1), \quad \zeta_2 = 2r .$$

Now the current output for the three regions can be written.

For S = 0:

$$y(x) = \frac{4x - 2z}{\pi z^2}\sqrt{x(z - x)} + \frac{1}{\pi}\sin^{-1}\left(2\frac{x}{z} - 1\right) + \frac{1}{2}$$

$$\text{for } 0 \leq x \leq z \qquad (71a)$$

$$y(x) = 1 \qquad \text{for } z \leq x \leq 1 \qquad (71b)$$

$$y(x) = -\frac{4(x-1) - 2z}{\pi z^2}\sqrt{(x - 1)(z - x + 1)} \qquad (71c)$$

$$- \frac{1}{\pi}\sin^{-1}\left(2\frac{x-1}{z} - 1\right) + \frac{1}{2} \quad \text{for } 1 \leq x \leq 1 + z$$

Figure 15 demonstrates y(x, S=0) for z = 0 and z = 0.4.

For $S \neq 0$ (using (73) and (74)):

$$y(x) = \frac{8(1 + S)}{\pi S^2 z^2}\left[S\sqrt{x(z - x)} + \sin^{-1}\left(1 - 2\frac{x}{z}\right) + \frac{\pi}{2}(T - 1)\right.$$

$$\left. - T\sin^{-1}\left\{1 - 2\frac{x}{z}(1 - Sz + Sx)\right\}\right] \quad \text{for } 0 \leq x \leq z \qquad (72a)$$

$$y(x) = \frac{8(1 + S)}{S^2 z^2}(T - 1) \qquad \text{for } z \leq x \leq 1 \qquad (72b)$$

$$y(x) = \frac{8(1 + S)}{\pi S^2 z^2}\left[-\frac{S+1}{S}\sqrt{(x - 1)(z - x + 1)} - \sin^{-1}\left(1 - 2\frac{x-1}{z}\right)\right.$$

$$\left. + T\sin^{-1}\left(1 - 2\frac{x-1}{z}\left\{1 - \frac{S}{1+S}(z-x+1)\right\}\right) + \frac{\pi}{2}(T - 1)\right]$$

$$\text{for } 1 \leq x \leq 1 + z . \qquad (72c)$$

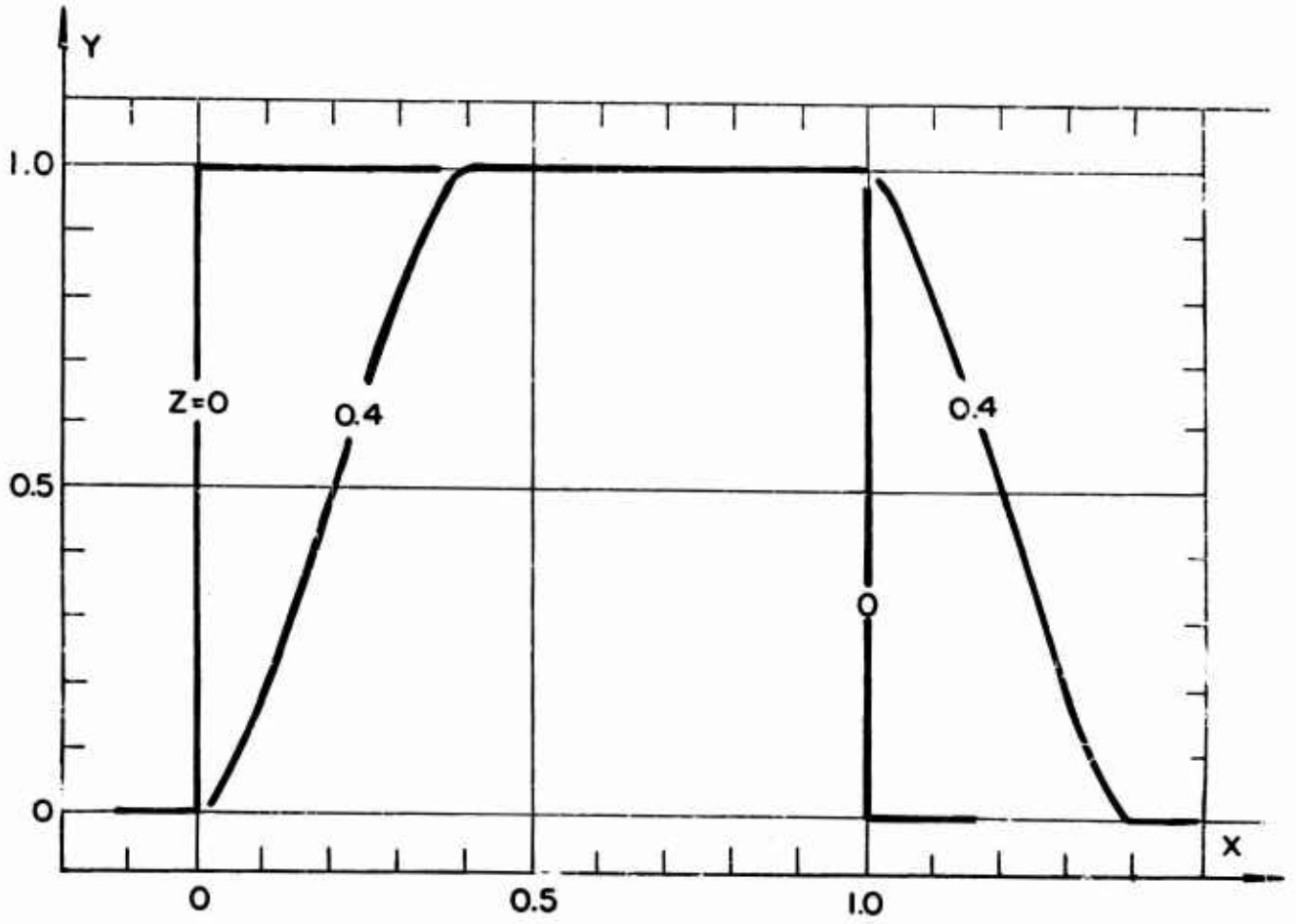

Figure 15. Influence of the angle of impact ($z \sim \tan \varphi$) on the curve shape (for $\epsilon_i = \epsilon_f$, R = L = 0)

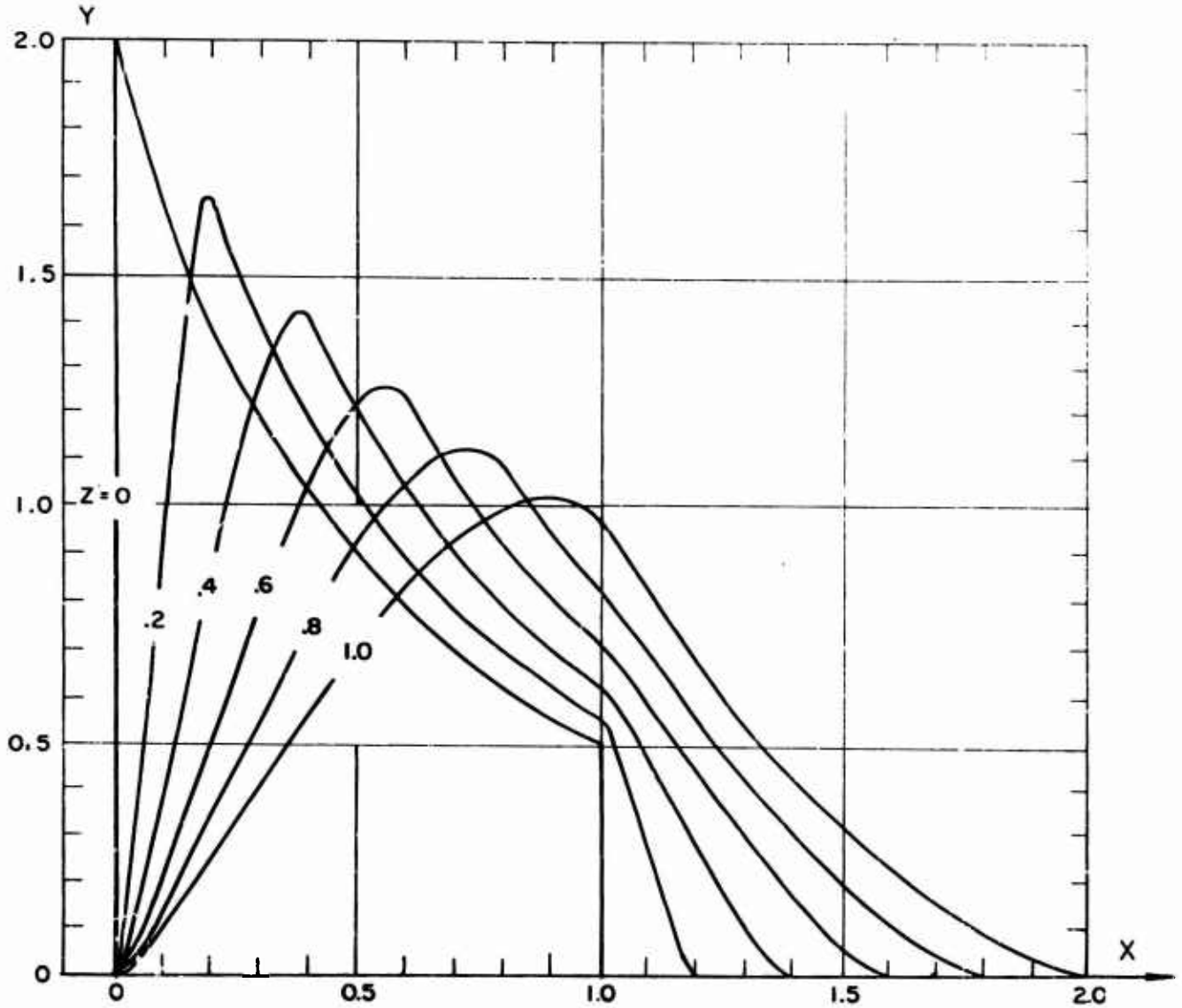

Figure 16. Influence of the angle of impact ($z=\tan\varphi$) on the curve shape (for $\epsilon_1 = 2\,\epsilon_f$, R = L = 0).

Figure 16 demonstrates $y(x, S = 1)$ for $z = 0, 0.2, 0.4, 0.6, 0.8, 1.0$.

8. THE SHORT-CIRCUIT ASSUMPTION

The mathematical treatment of many features (such as the curved hysteresis, maximum energy output, conductivity behind the shock front, oblique impact) is greatly facilitated or even only possible, if the short-circuit assumption $R = L = 0$ is made. Our experiments use an electric load $R = 10$ ohms and $L < 0.5 \cdot 10^{-7}$ henry, and the question has to be investigated whether the short-circuit formulas can be used with these values.

Figures 4 through 7 show how close curves with these values of R and L come to the limiting case $R = L = 0$. Only the initial part of the pulse, for $0 \leq t \leq 0.1 \cdot t_o$, is affected at all.

Another way of justifying the short circuit assumption with $R = 10$ ohms is to look at the element as a capacitor (capacitance $C = 7 \cdot 10^{-10}$ farad). With a short circuit the charge flows off immediately after it is set free (RC-time = 0). In our case the RC-time is $7 \cdot 10^{-9}$ sec, which is only 1 percent of the normal pulse duration $t_o = 7 \cdot 10^{-7}$ seconds.

A third way of showing that $R = 10$ ohms is small enough to justify the short-circuit assumption is to use equation (1). As the curves for small R show (fig. 5), for a time $x = 0.3$, (traveled distance $\xi = 0.1$ cm) about 50 percent of the total charge has flowed off the electrodes ($\sigma(0.3) = P_o/2$). At this moment the voltage between the shock front and the back electrode is approximately, according to equation (1):

$$\frac{\sigma - P_o}{\epsilon_i}(\ell - \xi) = -\frac{0.5P_o}{\epsilon_i}(\ell - \xi) = \frac{0.5 \cdot (8) \cdot 10^{-6}}{0.886 \cdot 10^{-10}}(0.22) = -9900 \text{ v}$$

At the same time the voltage between the shock front and the front electrode is approximately, according to equation (1):

$$\frac{\sigma}{\epsilon_f}\xi = \frac{0.5P_o}{\epsilon_f}\xi = \frac{0.5 \cdot (8) \cdot 10^{-6}}{0.443 \cdot 10^{-10}}(0.1) = 9100 \text{ v}$$

The current at this time is only about 25 amp (measured value), and the voltage across R therefore 250 v. This demonstrates that neglecting the third term in equation (1) does not introduce a big error.

9. METHODS FOR EVALUATING ϵ_f FROM EXPERIMENTAL DATA

The equations in the previous sections contain all or some of these values: A, ℓ, P_o, Q, t_o, R, L, ρ, α, β, φ, ϵ_i, and ϵ_f. If Q approaches $A \cdot P_o$, then the resistivity ρ is sufficiently high, as shown in section 6, and we need not correct for any current leakage through the compressed region. Then everything can be measured before or during the experiment, except ϵ_f. This quantity therefore is determined by the outcome of the experiment, i.e., the current output y(x) or I(t). ϵ_f is the dielectric constant of the material under high compression and elevated temperature, the temperature being determined along with the compression by the methods discussed in reference 1. ϵ_f is an important property of the material under those conditions, and it is one of the main objects of our present experiments to get values for ϵ_f. Most of the formulas of the preceding sections are too complicated to be solved for ϵ_f, and we have to look for the most simple expressions and elect the appropriate experimental arrangements. One of these is the open circuit situation

$$y(x) = \frac{\ell t_o}{\epsilon_f AR} x, \text{ from which follows}$$

$$U(t) = R \cdot I(t) = R \frac{Q_o}{t_o} y \left(\frac{t}{t_o}\right) = \frac{P_o \ell}{\epsilon_f t_o} t \quad \text{and}$$

$$\frac{dU}{dt} = \frac{P_o \ell}{\epsilon_f t_o} .$$

This, by the way, is the initial rise of U(t) for any R (equation 19) which for an open circuit goes on as a linear rise.

Equation (75) is very simple, and one need only measure the rise of the curve: voltage versus time. The difficulties however are:

1) Very high voltages are reached within a short time (with our experimental values: 60 kv at $t = t_o = 0.7$ μsec), which may generate breakdowns through the element, around the edges, and across the probes.

2) t_o is not easily found, since the actual scope traces of open-circuit experiments do not show a clear picture of the pulse and especially its end part.

3) Disturbances of the rise time, due to the angle of impact, to the amplifiers, or to any other reason, are superimposed and therefore falsify the resulting apparent value of ϵ_f.

It might, however, be possible to overcome these difficulties and to get proper results by this method.

The other simple arrangement is the short-circuit situation, which is treated in many details in this report, and which is nearly fulfilled in our experiments (see section 8). The rest of this section (9) deals with methods to evaluated ϵ_f from a given curve I(t) or y(x) under short circuit conditions.

Usually a curve U(t) is obtained, with a known value of R (10 ohms). Therefore I(t) is given. This curve generally shows a main pulse, past which the curve goes through the zero line. The current then becomes negative for a while, followed by a smaller pulse and ripples. The pulse, as far as we need it, is at its end at the crossover with the zero line. Everything that follows is influenced by reflections and is of no interest. The charge output is $Q = \int I\,dt$ across that main pulse, the experimental values of Q are close to Q_o, and are put equal to Q_o for the following calculations. The pulse never appears to be ideal, the rise and decay are not vertical but inclined lines, even where a small angle of impact has been measured. Therefore the normal pulse length t_o has to be taken between (a) the half value of the first straight line of the rise and (b) the half value of the decay of the pulse. This is in agreement with figures 8 through 10, which show that the rise of the curves consists of a first straight line, followed by a bend and a more inclined part. In figure 17, the important parts of the curve are identified.

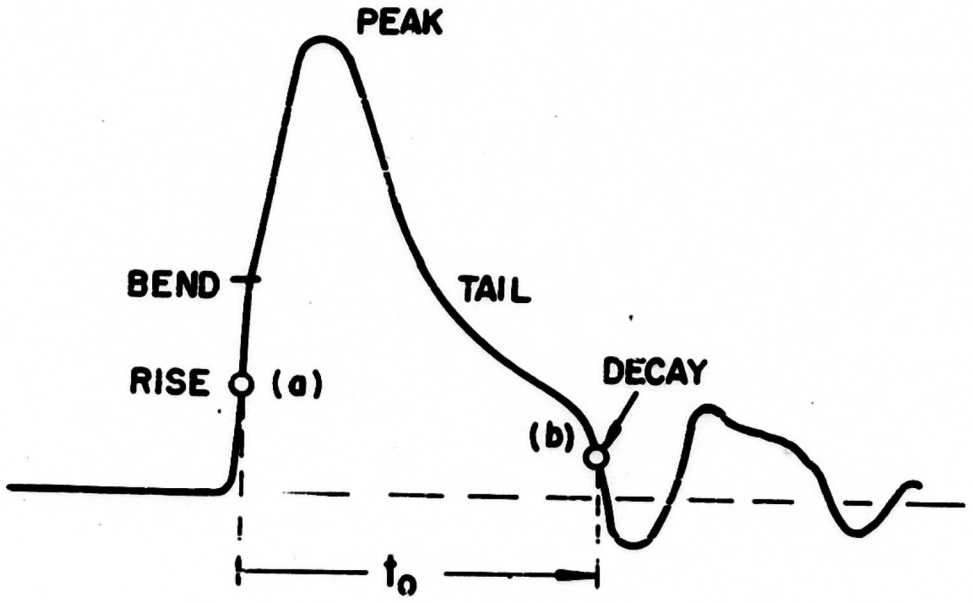

Figure 17. General pulse shape for short circuit.

With t_o and Q_o, the transformation to the normalized form $x = t/t_o$, $y = I \cdot t_o/Q_o$ can be made

Due to the deviation from the ideal curve shape, as stated before, the leading part of the pulse is not well suited to derive ϵ_f from it. The tail, however, follows closely the theoretical formulas except for the decay part of the pulse which also cannot be used. The quickest, although not very precise, method to evaluate ϵ_f appears by use of equation (10), which solved for $\epsilon_i/\epsilon_f = S + 1$ gives us:

$$\begin{cases} \epsilon_i/\epsilon_f = \left[1 - 2xy(1-x) - \sqrt{1 - 4xy(1-x)}\right] /2x^2y & \text{for } 0 < x \leq x_m \\ \epsilon_i/\epsilon_f = \left[1 - 2xy(1-x)\right]/2x^2y & \text{for } x = x_m \\ \epsilon_i/\epsilon_f = \left[1 - 2xy(1-x) + \sqrt{1 - 4xy(1-x)}\right] /2x^2y & \text{for } x_m \leq x \leq 1 \\ \epsilon_i/\epsilon_f = 1/y & \text{for } x = 1 \end{cases} \tag{76}$$

$$\text{with} \quad x_m = \frac{1}{2+S} = \frac{\epsilon_f}{\epsilon_i+\epsilon_f} \; .$$

ϵ_i is a mean value of the dielectric constant in the uncompressed material, as explained in section 1.

A better method is to use equation (34) instead of (10), thus employing the curved hysteresis instead of the linear fit. This brings us nearer to the actual pulse shape. In doing so, the quadratic fit α, β to the hysteresis curve (equation 4) must be known, instead of only the mean value ϵ_i. The general formula (34) cannot be solved analytically for ϵ_f, an approximate formula must be invented. This is done by creating an auxiliary function $\phi(x)$, which derives it justification solely from the fact that it approaches the tail of y(x) so closely, as can be seen in figures 8, 9, and 10.

A curve (similar to equation 10) $y(\bar{x}) = \dfrac{k}{\left[1+(k-1)\bar{x}\right]^2}$ for $0 \leq \bar{x} \leq 1$,

is transformed to the range $x_p \leq x \leq 1$ by the linear transformation $\bar{x} = \dfrac{x-x_p}{1-x_p}$, giving

$$y(\bar{x}) = \phi(x) = \frac{k(1-x_p)^2}{\left[1-kx_p + (k-1)\,x\right]^2} \; ,$$

The value of $\phi(1) = \frac{1}{k}$ is forced to coincide with $y(1) = \epsilon_f/\epsilon_m$ (from equation 34). This determines $k = \epsilon_m/\epsilon_f$ and thereby

$$\phi(x) = \frac{\frac{\epsilon_m}{\epsilon_f}(1-x_p)^2}{\left[1-\frac{\epsilon_m}{\epsilon_f}x_p + \frac{\epsilon_m-\epsilon_f}{\epsilon_f}x\right]^2} \quad \text{for } x_p < x \leq 1 \; . \tag{77}$$

x_p is the position of the peak of the curve y(x) according to equation (34). ϵ_m is defined with equation (34). Equation (77) can be solved for ϵ_m/ϵ_f, giving

$$\frac{\epsilon_m}{\epsilon_f} = \frac{1}{2\phi}\left(\frac{1-x_p}{x-x_p}\right)^2 \left\{1 + \sqrt{1-4\phi\,\frac{(1-x)(x-x_p)}{(1-x_p)^2}}\right\} - \frac{1-x}{x-x_p} \; . \tag{78}$$

By putting the values of x_p of ϵ_m and any values of x and y (the latter for ϕ) from along the tail of the measured and normalized output curve y(x) into equation (78), this equation yields ϵ_f. Figures 8, 9, and 10 show which part of the tail is suitable.

ACKNOWLEDGMENT

The author wishes to thank P. S. Brody for introduction into this field and for helpful discussions, and H. R. Kollmeyer who did most of the work for the experimental setup and helped carry out the experiments. R. F. Butler set up the analog computer which drew some curves for section 3. The work was supported as part of a Transducer Research Project.

REFERENCES

1) P. S. Brody, "Strong Shock Waves in 'Polled' Barium Titanate Ceramic Elements," DOFL Report TR-869 (October 20, 1960).

2) P. S. Brody, R. H. Wittekindt, "Dielectric Constant of Barium Titanate at 100 Kilobars," DOFL Report TR-917 (March 15, 1961).

3) R. Schall, K. Vollrath, "Zum Verhalten ferroelektrischer Keramik bei intensiven Stosswellen," Bericht über den IV. Internationalen Kongress fur Kurzzeitphotographie, Koln 1958, p 329.

4) E. Kamke, "Gewöhnliche Differentialgleichungen," Akadamische Verlagsgesellschaft, Leipzig (1943).

DISTRIBUTION

Department of the Army
Office of the Chief of Ordnance
The Pentagon, Washington 25, D. C.
Attn ORDTN (Nuclear & Special Components Branch)
Attn: ORDTB, Joseph Kaufman

Director, Army Research Office
Office of the Chief of Research & Development
Department of the Army
Washington 25, D. C.

Commanding Officer
Picatinny Arsenal
Dover, New Jersey
Attn: Feltman Research & Engineering Laboratories
Attn: Library

Commanding Officer
U.S. Army Signal Research & Development Laboratory
Fort Monmouth, New Jersey
Attn: Tech Library

Commanding General
Aberdeen Proving Ground, Maryland
Attn: BRL—R. J. Eichelberger

Commanding Officer
U.S. Army, Office of Ordnance Research
Box CM, Duke Station
Durham, North Carolina

Commanding General
Engineer Research & Development Laboratories
U. S. Army
Fort Belvoir, Virginia
Attn: Tech Documents Center

Commander
U.S. Naval Ordnance Laboratory
Corona, California
Attn: Documents Librarian

Commander
U.S. Naval Ordnance Laboratory
White Oak, Silver Spring 19, Maryland
Attn: M. Solow
Attn S. J. Jacobs
Attn: B. Drimmer

Department of the Navy
Bureau of Naval Weapons
Washington 25, D. C.
Attn: DLI-3--Tech Library

Commander
Naval Research Laboratory
Washington 25, D. C.
Attn: G. Irwin
Attn: Tech Library

Commander
Armed Services Technical Information Agency
Arlington Hall Station
Arlington 12, Virginia
Attn: TIPDR (10 copies)

Sandia Corporation
Sandia Base
Albuquerque, New Mexico
Attn: G. Anderson
Attn: F. Nielson
Attn: R. Grahm
Attn: H. G. Baerwald

Los Alamos Scientific Laboratory
Los Alamos, New Mexico
Attn: J. Wackerlee
Attn: J. M. Walsh
Attn: R. Duff
Attn: S. Minshall

University of California
Radiation Laboratory
Livermore, California
Attn: Taylor Abegge

Director, Stanford Research Institute
Menlo Park, California
Attn: The Poulter Laboratories

Clevite Research Corp
Cleveland,Ohio
Attn: H. Jaffe
Attn: D. Berlincourt

National Bureau of Standards
Mineral Products Division
Industrial Bldg.
Attn: A. D. Franklin

DISTRIBUTION (Continued)

National Bureau of Standards
Thermodynamics Division
West Building
Attn: M. S. Green

National Bureau of Standards
Mechanics Division
Industrial Building
Attn: E. C. Lloyd
Attn: L. K. Irwin

Internal

Hinman, W. S., Jr./McEvoy, R. W.
Apstein, M./Gerwin, H. L./Guarino, P. A./Kalmus, H. P.
Sures, A. H./Schwenk, C. C.
Hardin, C. D., Lab 100
Horton, B. M., Lab 200
Rotkin, I., Lab 300
Landis, P. E./Tuccinardi, T. E., Lab 400
Hatcher, R. D., Lab 500
Flyer, I. N., Lab 600
Campagna, J. H./Apolenis, C. J., Div 700
DeMasi, R., Div 800
Franklin, P. J./Horsey, E. F., Lab 900
Harris, F. T., 310
Bowles, R. E., 310
Brody, P. S., 310
Kinzelman, G. W , 320
Piper, W., 320
Ravitsky, C., 310
Warren, R., 310
Curchack, H., 310
Horn, L., 310
Wittekindt, R., 310 (20 copies)
Seaton, J. W., 260
Technical Reports Unit, 800 (3 copies)
DOFL Library (5 copies)
Technical Information Office, 010 (10 copies)

(Two pages of abstract cards follow.)

AD________ Accession No.________

DIAMOND ORDNANCE FUZE LABORATORIES, Washington 25, D. C.

SHAPE OF THE CURRENT OUTPUT PULSE FROM A THIN FERROELECTRIC CYLINDER UNDER SHOCK COMPRESSION - - R. H. Wittekindt

TR-922, 15 May 1961, 35 pp text, 17 illus., DA-5B97-01-005, OMS-5010.11.82600, DOFL Proj 30300, UNCLASSIFIED Report

When a polarized ferroelectric element is traversed by a shock front that destroys the polarization, a current output appears. The shape of the curve of this current output versus time is computed in a normalized and general form for the case where the shock front moves in a direction normal (or approximately normal) to the electrodes and parallel to the polarization. The influence of the external electric load, of the dielectric constants and the hysteresis, of a conductivity in the compressed material, and of an oblique impact is discussed. The condition for maximum energy output also is discussed. Mathematical expressions for the current output are given for the various conditions, examples are calculated and shown in graphs. Methods are described for evaluating the dielectric constant in the compressed material from measured output curves.

Shock waves

Theory

AD________ Accession No.________

DIAMOND ORDNANCE FUZE LABORATORIES, Washington 25, D. C.

SHAPE OF THE CURRENT OUTPUT PULSE FROM A THIN FERROELECTRIC CYLINDER UNDER SHOCK COMPRESSION - - R. H. Wittekindt

TR-922, 15 May 1961, 35 pp text, 17 illus., DA-5B97-01-005, OMS-5010.11.82600, DOFL Proj 30300, UNCLASSIFIED Report

When a polarized ferroelectric element is traversed by a shock front that destroys the polarization, a current output appears. The shape of the curve of this current output versus time is computed in a normalized and general form for the case where the shock front moves in a direction normal (or approximately normal) to the electrodes and parallel to the polarization. The influence of the external electric load, of the dielectric constants and the hysteresis, of a conductivity in the compressed material, and of an oblique impact is discussed. The condition for maximum energy output also is discussed. Mathematical expressions for the current output are given for the various conditions, examples are calculated and shown in graphs. Methods are described for evaluating the dielectric constant in the compressed material from measured output curves.

Shock waves

Theory

AD________ Accession No.________

DIAMOND ORDNANCE FUZE LABORATORIES, Washington 25, D. C.

SHAPE OF THE CURRENT OUTPUT PULSE FROM A THIN FERROELECTRIC CYLINDER UNDER SHOCK COMPRESSION - - R. H. Wittekindt

TR-922, 15 May 1961, 35 pp text, 17 illus., DA-5B97-01-005, OMS-5010.11.82600, DOFL Proj 30300, UNCLASSIFIED Report

When a polarized ferroelectric element is traversed by a shock front that destroys the polarization, a current output appears. The shape of the curve of this current output versus time is computed in a normalized and general form for the case where the shock front moves in a direction normal (or approximately normal) to the electrodes and parallel to the polarization. The influence of the external electric load, of the dielectric constants and the hysteresis, of a conductivity in the compressed material, and of an oblique impact is discussed. The condition for maximum energy output also is discussed. Mathematical expressions for the current output are given for the various conditions, examples are calculated and shown in graphs. Methods are described for evaluating the dielectric constant in the compressed material from measured output curves.

Shock waves

Theory

AD________ Accession No.________

DIAMOND ORDNANCE FUZE LABORATORIES, Washington 25, D. C.

SHAPE OF THE CURRENT OUTPUT PULSE FROM A THIN FERROELECTRIC CYLINDER UNDER SHOCK COMPRESSION - - R. H. Wittekindt

TR-922, 15 May 1961, 35 pp text, 17 illus., DA-5B97-01-005, OMS-5010.11.82600, DOFL Proj 30300, UNCLASSIFIED Report

When a polarized ferroelectric element is traversed by a shock front that destroys the polarization, a current output appears. The shape of the curve of this current output versus time is computed in a normalized and general form for the case where the shock front moves in a direction normal (or approximately normal) to the electrodes and parallel to the polarization. The influence of the external electric load, of the dielectric constants and the hysteresis, of a conductivity in the compressed material, and of an oblique impact is discussed. The condition for maximum energy output also is discussed. Mathematical expressions for the current output are given for the various conditions, examples are calculated and shown in graphs. Methods are described for evaluating the dielectric constant in the compressed material from measured output curves.

Shock waves

Theory

REMOVAL OF EACH CARD WILL BE NOTED ON INSIDE BACK COVER, AND REMOVED CARDS WILL BE TREATED AS REQUIRED BY THEIR SECURITY CLASSIFICATION.

AD________ Accession No.________

DIAMOND ORDNANCE FUZE LABORATORIES, Washington 25, D. C.

SHAPE OF THE CURRENT OUTPUT PULSE FROM A THIN FERROELECTRIC CYLINDER UNDER SHOCK COMPRESSION - - R. H. Wittekindt

TR-922, 15 May 1961, 35 pp text, 17 illus., DA-5B97-01-005, OMS-5010.11.82600, DOFL Proj 30300, UNCLASSIFIED Report

Shock waves

Theory

When a polarized ferroelectric element is traversed by a shock front that destroys the polarization, a current output appears. The shape of the curve of this current output versus time is computed in a normalized and general form for the case where the shock front moves in a direction normal (or approximately normal) to the electrodes and parallel to the polarization. The influence of the external electric load, of the dielectric constants and the hysteresis, of a conductivity in the compressed material, and of an oblique impact is discussed. The condition for maximum energy output also is discussed. Mathematical expressions for the current output are given for the various conditions, examples are calculated and shown in graphs. Methods are described for evaluating the dielectric constant in the compressed material from measured output curves.

AD________ Accession No.________

DIAMOND ORDNANCE FUZE LABORATORIES, Washington 25, D. C.

SHAPE OF THE CURRENT OUTPUT PULSE FROM A THIN FERROELECTRIC CYLINDER UNDER SHOCK COMPRESSION - - R. H. Wittekindt

TR-922, 15 May 1961, 35 pp text, 17 illus., DA-5B97-01-005, OMS-5010.11.82600, DOFL Proj 30300, UNCLASSIFIED Report

Shock waves

Theory

When a polarized ferroelectric element is traversed by a shock front that destroys the polarization, a current output appears. The shape of the curve of this current output versus time is computed in a normalized and general form for the case where the shock front moves in a direction normal (or approximately normal) to the electrodes and parallel to the polarization. The influence of the external electric load, of the dielectric constants and the hysteresis, of a conductivity in the compressed material, and of an oblique impact is discussed. The condition for maximum energy output also is discussed. Mathematical expressions for the current output are given for the various conditions, examples are calculated and shown in graphs. Methods are described for evaluating the dielectric constant in the compressed material from measured output curves.

AD________ Accession No.________

DIAMOND ORDNANCE FUZE LABORATORIES, Washington 25, D. C.

SHAPE OF THE CURRENT OUTPUT PULSE FROM A THIN FERROELECTRIC CYLINDER UNDER SHOCK COMPRESSION - - R. H. Wittekindt

TR-922, 15 May 1961, 35 pp text, 17 illus., DA-5B97-01-005, OMS-5010.11.82600, DOFL Proj 30300, UNCLASSIFIED Report

Shock waves

Theory

When a polarized ferroelectric element is traversed by a shock front that destroys the polarization, a current output appears. The shape of the curve of this current output versus time is computed in a normalized and general form for the case where the shock front moves in a direction normal (or approximately normal) to the electrodes and parallel to the polarization. The influence of the external electric load, of the dielectric constants and the hysteresis, of a conductivity in the compressed material, and of an oblique impact is discussed. The condition for maximum energy output also is discussed. Mathematical expressions for the current output are given for the various conditions, examples are calculated and shown in graphs. Methods are described for evaluating the dielectric constant in the compressed material from measured output curves.

AD________ Accession No.________

DIAMOND ORDNANCE FUZE LABORATORIES, Washington 25, D. C.

SHAPE OF THE CURRENT OUTPUT PULSE FROM A THIN FERROELECTRIC CYLINDER UNDER SHOCK COMPRESSION - - R. H. Wittekindt

TR-922, 15 May 1961, 35 pp text, 17 illus., DA-5B97-01-005, OMS-5010.11.82600, DOFL Proj 30300, UNCLASSIFIED Report

Shock waves

Theory

When a polarized ferroelectric element is traversed by a shock front that destroys the polarization, a current output appears. The shape of the curve of this current output versus time is computed in a normalized and general form for the case where the shock front moves in a direction normal (or approximately normal) to the electrodes and parallel to the polarization. The influence of the external electric load, of the dielectric constants and the hysteresis, of a conductivity in the compressed material, and of an oblique impact is discussed. The condition for maximum energy output also is discussed. Mathematical expressions for the current output are given for the various conditions, examples are calculated and shown in graphs. Methods are described for evaluating the dielectric constant in the compressed material from measured output curves.

REMOVAL OF EACH CARD WILL BE NOTED ON INSIDE BACK COVER, AND REMOVED CARDS WILL BE TREATED AS REQUIRED BY THEIR SECURITY CLASSIFICATION.